MODEL STUDIES ON MIXING AND HEATFLOW IN ELECTRO SLAG REFINING

by

ANTOJOY PULIKKOTTIL

DEPARTMENT OF METALLURGICAL ENGINEERING

INDIAN INSTITUTE OF TECHNOLOGY, KANPUR

SEPTEMBER, 1987

MODEL STUDIES ON MIXING AND HEATFLOW IN ELECTRO SLAG REFINING

A Thesis Submitted
In Partial Fulfillment of the Requirements
for the Degree of

MASTER OF TECHNOLOGY

by
ANTOJOY PULIKKOTTIL

to the

DEPARTMENT OF METALLURGICAL ENGINEERING

INDIAN INSTITUTE OF TECHNOLOGY, KANPUR

SEPTEMBER, 1987
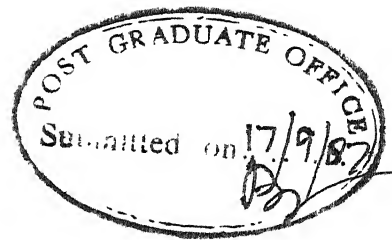
669.14

P966m

ME-1987-M-PUL-MOD

dedicated to

my   parents

CERTIFICATE

Certified that this work on 'Model Studies on Mixing
and Heat Flow in Electro Slag Refining' has been carried out
by Anto Joy P. under my supervision and that it has not been
submitted elsewhere for a degree.

(N.K. Batra)
Professor
Department of Metallurgical Engineering
Indian Institute of Technology
Kanpur.

ACKNOWLEDGEMENTS

CONTENTS

List of Tables

List of Figures

ABSTRACT

Laboratory studies have been conducted using the low
melting point systems of NH_4Cl solution in water and pure
$ZnCl_2$, and the mixing and heat flow patterns in the liquid bath
have been studied by measuring the temperature responses at
different locations of the bath, temperature and flow rates of
the cooling water passed and the voltage and the current
supplied to heat the bath. A few experiments were conducted
using nonconsumable copper electrodes in the NH_4Cl-H_2O system
and pure $ZnCl_2$ system and some using consumable lead electrodes
in the pure $ZnCl_2$ bath held in a water cooled double walled copper
mould as to simulate the conditions encountered in the electro-
slag refining of metals. The paths of the current flow in the
liquid bath were varied by insulating the mould walls in
the case of NH_4Cl-H_2O solution and the copper electrode in the
case of $ZnCl_2$ bath. The lead electrode could be lowered into the
bath in steps of 6 mm at regular time intervals of 30 sec. The
results show that heating and mixing of the noninsulated bath
using non-consumable copper electrode are confined up to the
depth of the electrode immersion due to the shorter distance of
current flow. Thermal convections are not set up in this case
as the colder liquid bath lies at the bottom. The cooling of
the mould walls by the flow of water increases the severity of
non-uniformity of the temperature in the bath. Insulation of the
mould walls or the electrode results in enhanced stirring of the

bath leading to its more uniform heating. In such cases the
current tends to flow from the electrode to the base of the
mould and the thermal convections are set up in the bath. The
formation of a solidified slag layer on the inner sides of the
mould walls leads to uniform heating of the bath due to the
same reason as given above. These conditions of skin formation
are obtained by manual stirring of the bath prior to the passing
of the cooling water and lowering the lead electrode, Otherwise
the $ZnCl_2$ bath at the bottom most layer tends to solidify as
soon as the cooling water is passed in the annular space of the
mould and the flow of current as well as heating of bath is
restricted to the upper region of the bath as long as complete
skin of solidified mass is not formed.

CHAPTER I

INTRODUCTION

1.1 Process of Electroslag Refining

Electro slag refining is a method of refining metals,
using a molten slag that is electrically resistance heated.
The schematic diagram of the process is shown in Fig. 1.1.
The metal to be refined is in the form of an electrode,
which is suspended in a bath of molten slag contained in a
water cooled mould. The required heat is generated by an
electric current flowing between the electrode and the condu-
cting base on which the mould stands, the slag bath providing
the resistance element in the circuit. The melt rate and the
heat transfer are influenced by the fact that whether AC or
DC power is being used to heat the slag bath. Melt rate in
the case of DC electrode positive may be almost the same as
in the case of AC, whereas in the case of DC electrode
negative, melting rates are reported to be lower.[1] As the
slag temperature rises above the melting point of the metal,
the tip of the electrode melts to form a film of molten metal
or a droplet and gets refined by its contact with the slag.
It gets further refined when it gets detached from the
electrode tip and falls through the slag and is collected in
a pool below. Additional refining can occur at the slag-metal
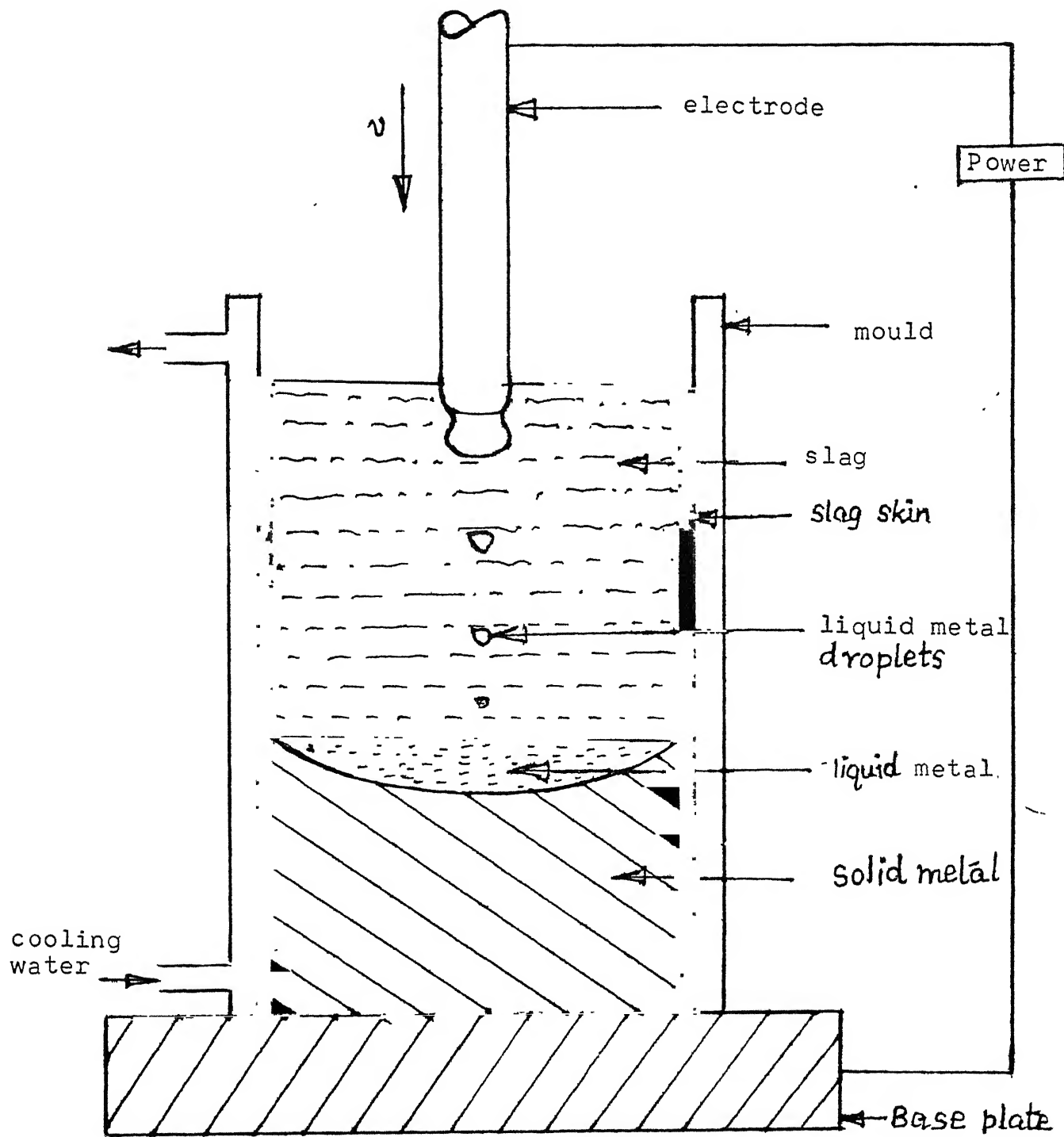
Fig. 1.1   Schematic drawing of electro-slag refining

pool interface before it solidifies. The surface of the slag bath is constantly being displaced upwards as the electrode is lowered and the process of refining continues. Kinetic factors for the refining reactions are favourable as the thin film of the molten metal in contact with the slag gives a very short diffusion path for the transport of reacting materials and products, as well as for the non-metallic material from the metal phase to the slag phase. Though some of these chemical aspects of refining may now be achieved more cheaply in the newer ladle or secondary steel making processes such as vacuum degassing, Argon Oxygen decarburizing of steel, injection metallurgy,etc, they cannot match the electro slag refining process in obtaining the structural benefits. A solidified skin of the slag adjacent to the mould walls eliminates the use of any refractories and contaminations by the erosion of the same and results in an excellent surface finish of the product steel.

The freezing operation takes place progressively as heat is removed from the metal via the base plate and via the mould walls by the circulation of cooling water in the annular space of the mould walls. By careful matching of the melt rate to the freezing rate, optimum conditions can be established to give excellent and desired ingot structure. As a result of the above factors, improved properties of steel such as high tensile strength, hot ductility, hot workability, good fracture toughness,

superior corrosion behaviour, reduced crack formation after welding etc. are easily attainable by the ESR process at lower costs.

1.2 Functions and Properties of Slag Bath

In the electro slag refining process described above, the importance of the liquid slag cannot be under rated. The functions of the liquid slag in the process are summarised as follows :

1. It acts as the heating element
2. It acts as a solvent for non-metallic materials
3. It is the refining agent of the process
4. It protects the metal from any atmospheric contamination
5. It acts as a transfer medium for the reactive components to be added to the alloy
6. It provides a lining to the mould to enhance the surface properties and smoothness of the ingot produced.

To meet the above stated functions, the slag must have the following properties.

1. Its melting temperature should be below that of the metal being melted and refined
2. Its operating temperature must be higher than that of the metal melting point
3. It should be possible to adjust the electrical resistivity of the slag within limits without adversely affecting the chemical requirements of the slag.

4. The composition should be such that the desired reactions can take place rapidly, and the reaction products are either retained in the slag or as in the case of sulphur, discharged into the atmosphere

5. It is important to select a slag that will suppress unwanted reactions such as the removal of essential trace elements

6. Viscosity affects the residence time of the metal droplets in the slag, the rate of escape of gases, the degree of stirring in the slag, the kinetics of mass transfer and the thickness of the slag crust formed. A slag of low viscosity at the operating temperature is preferred.

7. The difference in the density between the slag and the metal also has an effect on the residence time and size of droplets and it can play an important role in the selection of slags.

8. The interfacial tension between the slag and the metal [1] should have a low value, as to increase the mass transfer rate and facilitate the production of small droplets, but this can also reduce the tendency of slag and metal to separate and therefore increase the risk of slag entrapment.

Normally the low melting point eutectic of 59 wt % LiCl, 41 wt % KCl is used for refining of metals such as lead, zinc, aluminium and copper[1] while CaF_2 based flexes contained upto 20-25% lime and or 25 wt % Al_2O_3 or TiO_3 are commonly used for refining different grades of steel.[2]

1.3   Applications of Electro slag Refining

From the simple process implied by the brief descriptions given so far, a complex technology has evolved with far reaching effects in the modern civilization in the form of manufacturing components for the air, space and submarine vehicles, nuclear power equipment and military uses.   In addition to the simple production of ingots, there is   now a wide variety of allied processes such as electro-slag casting, electro-slag hot topping, central zone refining, ingot joining, electro-slag welding, electro-slag smelting etc.

While the primary purpose of ESR is to provide ingots for subsequent working, many variants have evolved. The excellent as-cast structure and high density mean that no hot work is required to take full advantage of the properties; so the material can be used in the as-cast condition.

The process has found wide-spread uses in the following :

1.   A major application for large ingots is in the production of rotors, for example, 12% Cr martensile steel [2]. In many cases these are subjected to both high and low temperature stress, and close control of composition and structure is required. ESR can meet all these requirements, and has the added advantage of increased yield, and reduced need for hot work, permitting a smaller ingot to be used than with conventional methods.

2. Many applications of ESR call for flat products, for
   example, marine, submarine, air and military vehicles,
   pressure vessels etc. The capability of producing
   rectangular ingots for such purposes has been counted as
   a point in favour of ESR in competition with other
   consumable electrode processes that are restricted to
   round ingots.[3]

3. A relatively high proportion of the output of installed
   capacity is used for the production of rolls.[5] The field
   of application most usually considered for ESR rolls is
   that of cold-mill work rolls as foil rolls, i.e., the
   products that have traditionally been made by forging and
   heat treatment.[5] ESR material can meet all the requirements,
   together with improved macro homogeneity and structure.[3]
   Worn rolls can be used directly as electrodes for ESR.
   Because of the improved density fine dendrite structure
   and absence of inclusions, porosity and micro segregation,
   the properties of as-cast ESR material are perfectly suita-
   ble for roll making without hot working.[4]

4. Roll cladding - Considerable attention has been given to
   the roll cladding operation which can be used either for
   the reclamation of worn rolls or for new rolls. ESR offers
   the possibility of using more highly alloyed materials for
   the shell, with the required metallurgical properties
   without increasing the cost.[5]

1.4 Scope of the Present Investigation

It may be noted from the discussion so far that the heat transfer and mixing in the ingot pool and the slag are important to study as they determine the degree of refining in the final ingot structure. For example, a deep metal pool would give rise to radial solidification of the metal whereas a flat and shallow pool is characterised by the axial heat flow. The pool depth may be controlled by the melt rate of the electrode, a high melt rate giving a deep metal pool and vice versa.[3] Many investigators have looked at this problem from the theoretical as well as from the practical considerations. It is now accepted that most of the heat is transferred to the metal pool via the falling metal droplets.[1] This was proved by the fact that the average depths of the metal pool using nonconsumable electrodes are only one quarter of pool depth obtained with consumable electrodes.

A complete literature survey covering these aspects of the problem are given in the next chapter.

Experiments have been carried out in the present work using NH_4Cl-H_2O solution and liquid $ZnCl_2$ bath with copper as well as lead electrodes to enhance the understanding of the heating patterns and mixing of the slag bath due to the flow of current by measuring the temperature responses at different locations of the bath, under varying experimental conditions. The outlines and plan of the work are described in Chapter III and the details

of the experiments carried out and the results obtained are given in Chapter IV and Chapter V respectively. Chapter VI gives the discussions and evaluations of the results obtained. The conclusions of the present work are given in Chapter VII. The recommendations for further work are given in Chapter VIII. A comprehensive list of the references and the literature cited for the work are given at the end of the thesis.

CHAPTER II

LITERATURE SURVEY

In this chapter the studies carried out by different investigators on the heat flow in the electrode, ingot as well as heat flow and mixing in the slag layer are reported.

2.1 Heat Flow in Electrodes

The amount of heat flowing out of the ESR process through the electrode may be important to study due to the following factors :

1. It influences the heat balance and hence the rate of melting in the electrode tip region.

2. It determines the temperature of the electrode material above the slag/gas interface and thus the amount of possible electrode oxidation.

3. It determines the extent to which the second phase particles dissolve before melting the matrix, i.e., determined by the time temperature correlations of the electrode material.

Mathematical models to represent and determine the temperature profiles within the electrode were put forward by Mitchel [6], Maulvault [7] and Mendrykowski [8]. Mitchel [6] considered the two dimensional temperature distribution in a cylindrical electrode above the slag level. In this formulation account was taken of

both the convective and the radiative heat transfer, to the electrode, but the effect of the actual vertical movement of the electrode did not appear explicitly. Heat transfer below the slag level was not taken into consideration. The investigation by Michel and coworkers made available extensive temperature measurements within the electrode which could be adequately reproduced by the model through the use of fitted parameters. Both the analysis and the measurements indicated that for small electrodes (20-50 mm dia), the radial temperature gradients are unlikely to be important, especially above the slag level.

Maulvault and Elliott[9] proposed a much simpler model for representing the axial temperature profile in small laboratory scale ESR units. Based on the experience of the research workers concerned with the simulation of the graphite electrodes in arc-furnaces, they assumed one dimensional heat flow, by taking into account the vertical movement of the electrode. Under steady state condition, Maulvault[7] arrived at the following :

$$\frac{d}{dZ}\left(k_s \frac{dT}{dZ}\right) - \frac{d}{dZ}\left(\rho\, C_s\, V_E T\right) = 0 \qquad (2.1)$$

where k_s is the thermal conductivity of the electrode material,

C_s is the specific heat of the electrode material,

ρ is the density of the electrode material,

and V_E is the melting speed of the electrode.

By the application of proper boundary conditions, the following solution was obtained :

$$\frac{T - T_E}{T_{me} - T_E} = \exp(-\frac{\rho C_s V_E}{K_s} Z) \quad \text{for} \quad Z < 0 \tag{2.2}$$

where T_E is the temperature of the upper part of the electrode and T_{me} is the temperature at the solid end of the electrode. The temperature profile along the center-line of the electrode for this model is given in Fig. 2.1. It was found that the predictions based on this very simple model were in reasonable agreement with the measurements carried out on a laboratory scale ESR unit, with an electrode dia of 37 mm. The results showed that the heating of the electrode is confined to the region 1-2 cm above the tip of the electrode at the same velocity *as* encountered in the ESR process.

Mendrykowski[8] proposed a more realistic one dimensional model for representing heat transfer in small, laboratory scale ESR units. The actual model is represented in Fig. 2.2 [8] where it may be noted that the electrode has been divided into four zones, i.e., i) radial and convection zone above the slag level, ii) zone of slag crust around the electrode, iii) zone of electrode dipped in the molten bath, iv) electrode tip. The heat transfer process within the electrode was represented by the following one dimensional heat conduction equation.
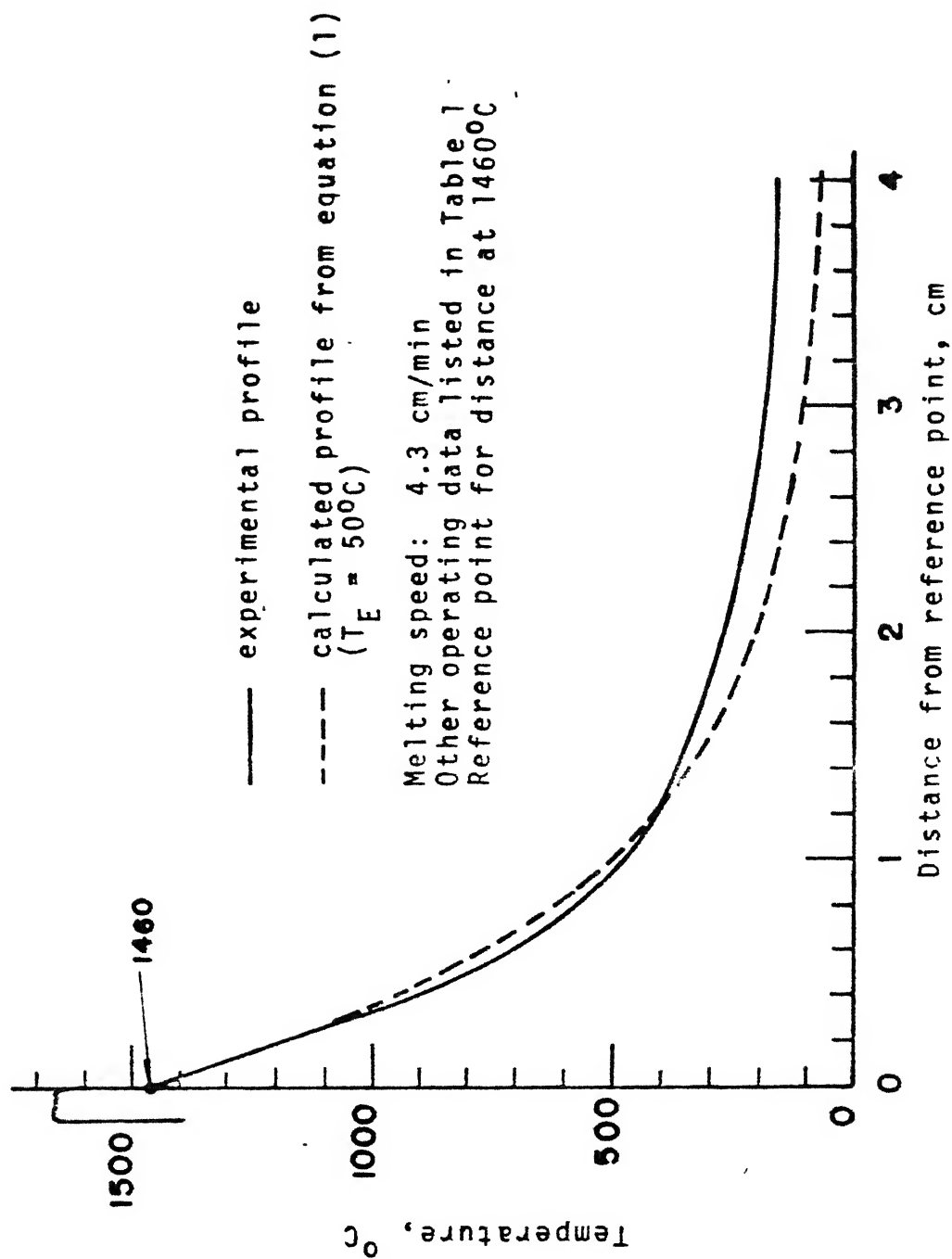
Figure 2.1. - temperature profile along center line of electrode.
Maulvault's model
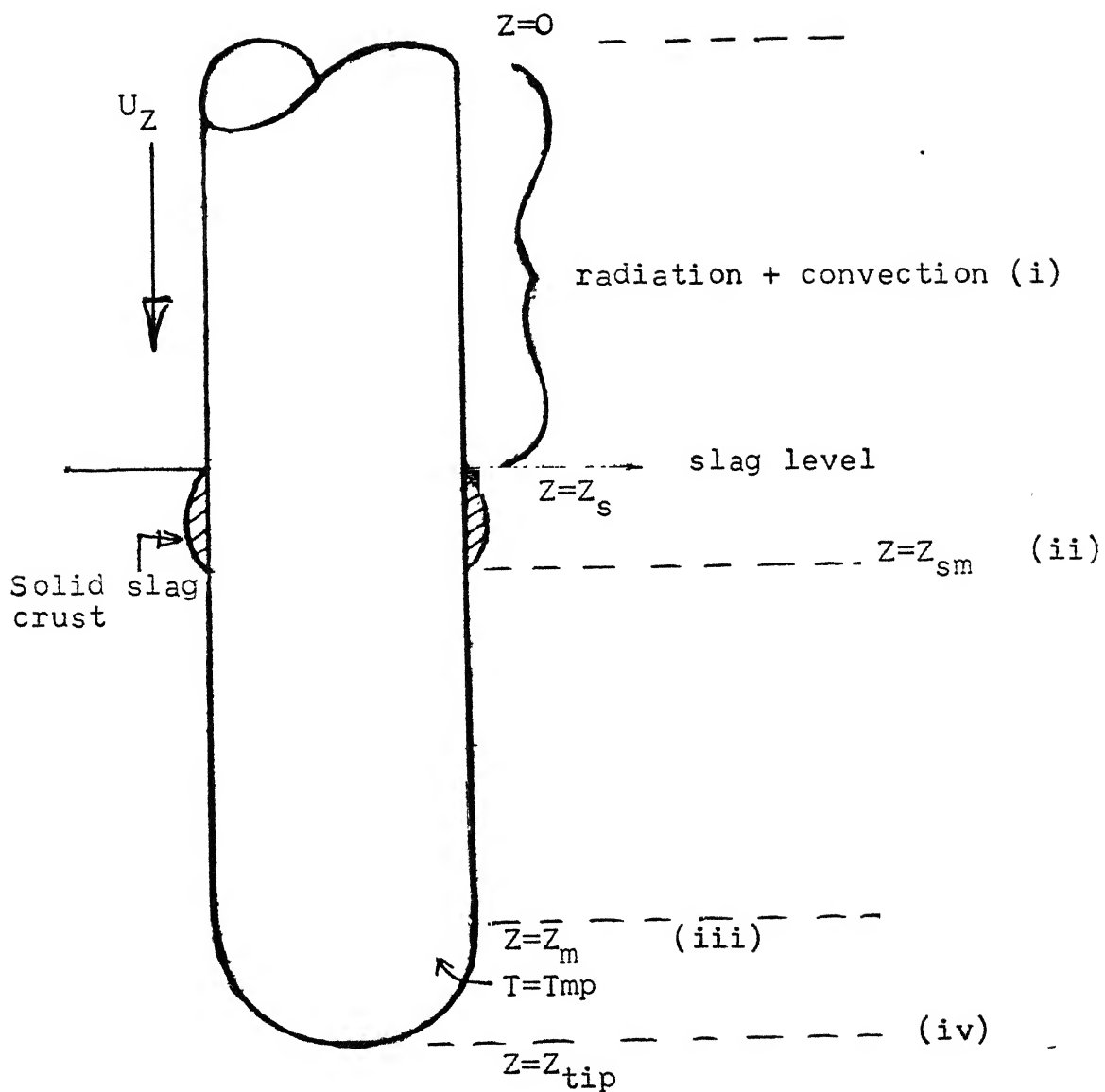
Fig. 2.2   Schematic diagram of electrode melting;
a model by Mendrykowski

$$K \frac{d^2T}{dZ^2} - \rho C_p U \frac{dT}{dZ} = -\frac{2}{R} q \quad \text{where} \qquad (2.3)$$

K is the thermal conductivity of the electrode material

T is the temperature of the electrode

U is the rate of travel of the electrode

R is the radius of the electrode

C_p is the specific heat of the electrode material

and q is the net heat flux.

Equation (2.3) is very similar to the expression used by Maulvault and Elliott,[9] except for the fact that the quantity q had to be different for each of the zones, reflecting the different heat transfer mechanisms prevailing in those regions. While the radiative and convective heat transfer contribution above the slag level were found relatively unimportant, the convective heat transfer between the slag and the electrode together with the conduction along the electrode were found to be important.

2.2 Heat Flow in Ingots

Heat transfer studies in the solidified ingot are of very complex nature and solutions are made possible under certain assumptions and simplifications.

Sun and Pridgeon[10] used the finite difference technique to determine the isothermal surfaces in the solidifying ingot of the 'Hastealloy - X' material. The overall mould/slag skin/ ingot interface heat transfer coefficient was first determined

experimentally by immersing the cold copper block in the liquid slag before using the same in the model.

Carvajal and Geiger[11] developed a model to simulate the freezing of an alloy with a long melting range. This model takes into account the variation in the thermal properties of the ingot material and with temperature at the surface. Paton[12] paid attention to the refinement of the boundary conditions in developing the mathematical model. Joshi[6] applied a numerical solution to the model which was similar to that of Sun, by measuring the boundary conditions experimentally. The temperature distribution of the ingot near the slag/ingot interface was determined by assuming an average temperature difference of 30 $^{\circ}$C between the slag and the metal. The heat balance of the process, obtained for the model by integrating the surface heat flows agreed well with the experimental measurements on small ingots (80-100 mm dia). Joshi[6] established that the effective thermal conductivity of the liquid pool is a significant parameter in determining the isotherm shape. He concluded that the 'best-fit' conductivity was about twice the true conductivity.

Maulvault[7] critically analyzed the effects of several approximations that have been used in modelling on the temperature profiles in ESR ingots. He used the relaxation technique[13] for the solving the complex heat balance equation and studied the effect of the effective thermal conductivity of the liquid

on the depth of the liquid pool. For a 500 mm dia ingot and the temperature of the top of the pool set at 1600 ^{O}C, he found that the calculated depth of the pool changed only slightly as the thermal conductivity was changed by a factor of 50; but increased rapidly with higher values. Maulvault used the model to calculate the ratio of pool depth to ingot radius, based on an assumed effective thermal conductivity of the liquid steel.

2.3 Mixing and Heat Flow in Slags

The slag bath may be in a state of motion due to the thermal convection effects and, more particularly due to electromagnetic effects, which are dependent on the current being passed and the electrode diameter. Viscosity of the slag is also an important factor. Generally speaking a quiescent bath can be obtained under conditions of high fill ratio (ratio of electrode dia to the mould dia) and high viscosity [3]. Under these conditions the high temperature zone immediately beneath the electrode may remain relatively undisturbed, giving optimum conditions to melt and superheat the metal.

The phenomenon of the slag motion has been studied by many investigators by employing the transparent moulds, low melting point systems of slags and metals or the electrical analogues. Campbell[1] and later Rawson[14] used fused salts with aluminium and graphite electrodes and demonstrated a torroidal stirring action shown in Fig. 2.3[1]. Slag streaming downwards from the electrode tip at a velocity that increased with decrease in the electrode

COOL
BOUNDARY
LAYER

HOT SLAG

COOL
BOUNDARY
LAYER

METAL POOL

SOLIDIFIED INGOT
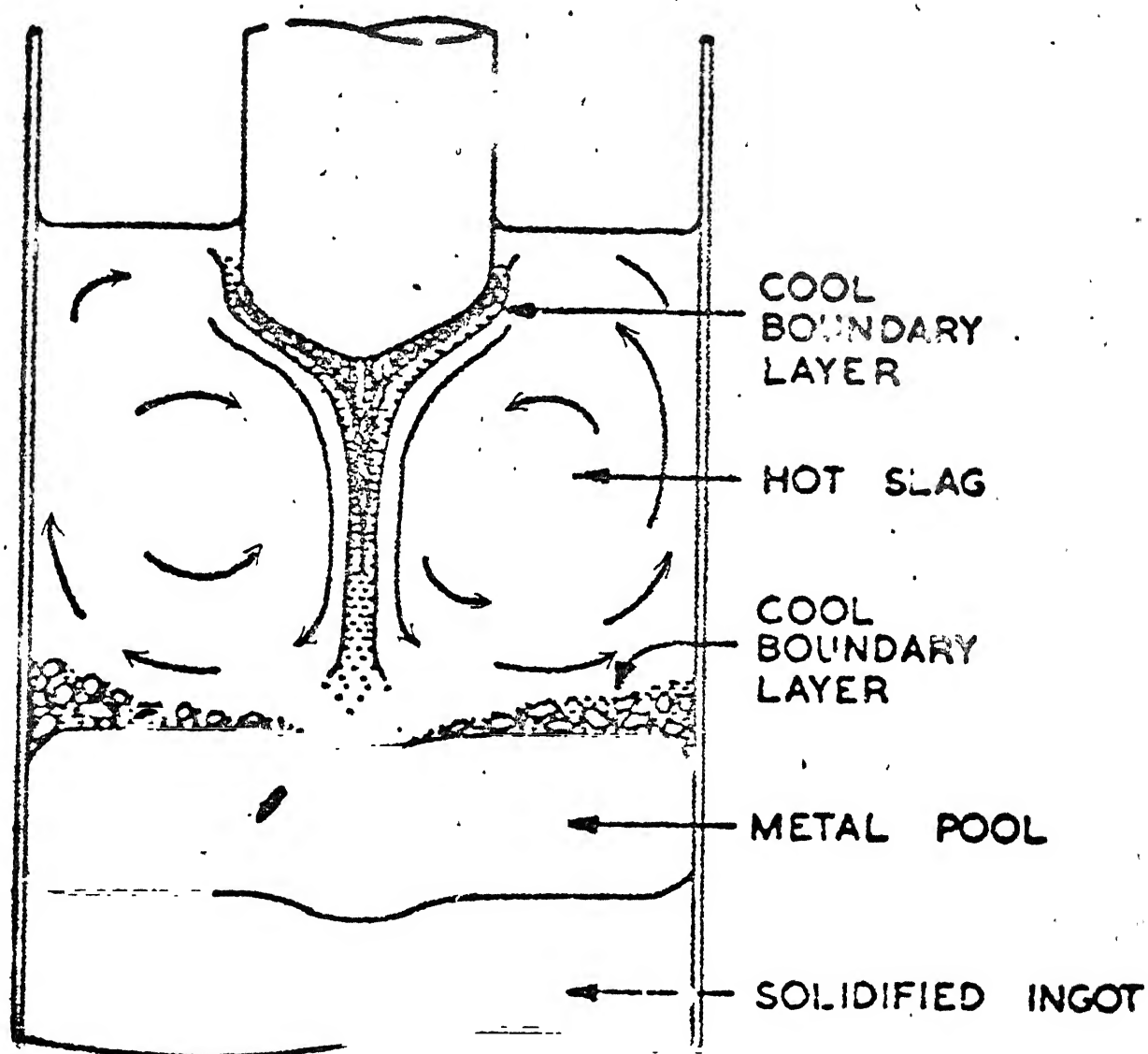
Fig. 2.3 Temperature distribution in slag layer, transparent model.

diameter with consumable and nonconsumable electrodes. With consumable electrode an increase in the velocity was observed during the period of formation of the droplet, due to the increased current as a result of decrease in the distance between the electrode and the base and due to the decrease in the dia of the electrode at the tip. Campbell[1] observed cool zones directly under the consumable electrode and at the periphery of the slag/ingot interface. The observation of the cool zone under the electrode seems to be in conflict with previously mentioned observations of the hot zone at this point. A possible explanation is that the slag has maximum resistivity at this point, and therefore maximum heat generation but, because it causes metal to melt, it is inevitably cooled by the heat exchange involved.

Rawson[14] extended Campbell's work to cover the slab melts, three phase and single phase power supply and bifilar systems.[4] The bifilar system gave superior heat generation in the viscinity of the electrodes, but a thicker slag skin. The results were confirmed by the electrical analogue work using a conductive paper and determining iso-voltage lines in a two dimensional model. In the case of the three-dimensional phase slab melting, it was concluded that the rapid changes in direction of stirring forces could not be accommodated, and the only significant stirring resulted from those forces which did not change direction as the phase changed.

2.4 Heat Balance in the ESR Process

An overall heat balance in the electro slag refining has been reported by many workers. The main source of heat is the Joule heating of the slag by the passage of the current, which is dissipated as follows :

1. Heat consumed in melting of the electrode material, i.e.,

$$Q_m = S_E \ V_E \ (H_{TS1} - H_{TO}) \rho_E$$

where S_E is the cross sectional area of the electrode, V_E is the velocity of electrode movement and H_{TS1} and H_{TO} are the enthalpies of metal at temperatures T_{S1} (temperature of the surface of the slag in the annular space between the electrode and the mould) and TO respectively.

2. Heat lost by conduction to the ingot below.

3. Heat lost to the cooling water passed through the annular space of the mould walls. This can be obtained by finding out the difference.

4. Heat lost to the surroundings by radiation

$$Q_R (Cal/sec) = \pi (R_m^2 - R_E^2) \ \varepsilon_s \sigma \ (T_{SS1}^4 - T_O^4)$$

where ε_s is the emissivity of the slag and σ is the stefan Boltzman constant, 1.356×10^{-12} Cal/cm^2/sec/$^{\circ}$K^4, and T_{SS1}, the temperature of the surface of the slag in the annular space between the electrode and the mould, TO, the temperature of

the surrounding and R_E and R_m are the radii of the electrode and the mould respectively.

The computed values of the heat losses by Choudhary and Szekely[15] and Maulvault[7] are compared in Table 2.1. The actual values measured in practice vary according to the design of the plant, the melting mode and the melt rate. In simple terms it may be considered that the heat balance is built up of two components; a steady component representing the equilibrium between the slag and its surroundings, and a variable component representing the heat used in melting the metal. The conditions at the slag/mould wall interface were studied by Mitehell and Joshi[2]. The temperature gradient across the slag bath/slag skin/ air-gap/mould wall is shown in Fig. 2.4.[2] The interface between the slag skin and the mould wall offers maximum resistance to heat flow.

TABLE 2.1 : Comparison of heat balance - ESR process

	Heat lost to the mould %	Heat lost to the electrode %
Chaudhary & Szekely	59	18.2

	Heat lost to electrode %	Heat lost to ingot %	Heat lost to cooling water %	Radiation heat loss %
Maulvault	27.8	32.8	34.8	4.6
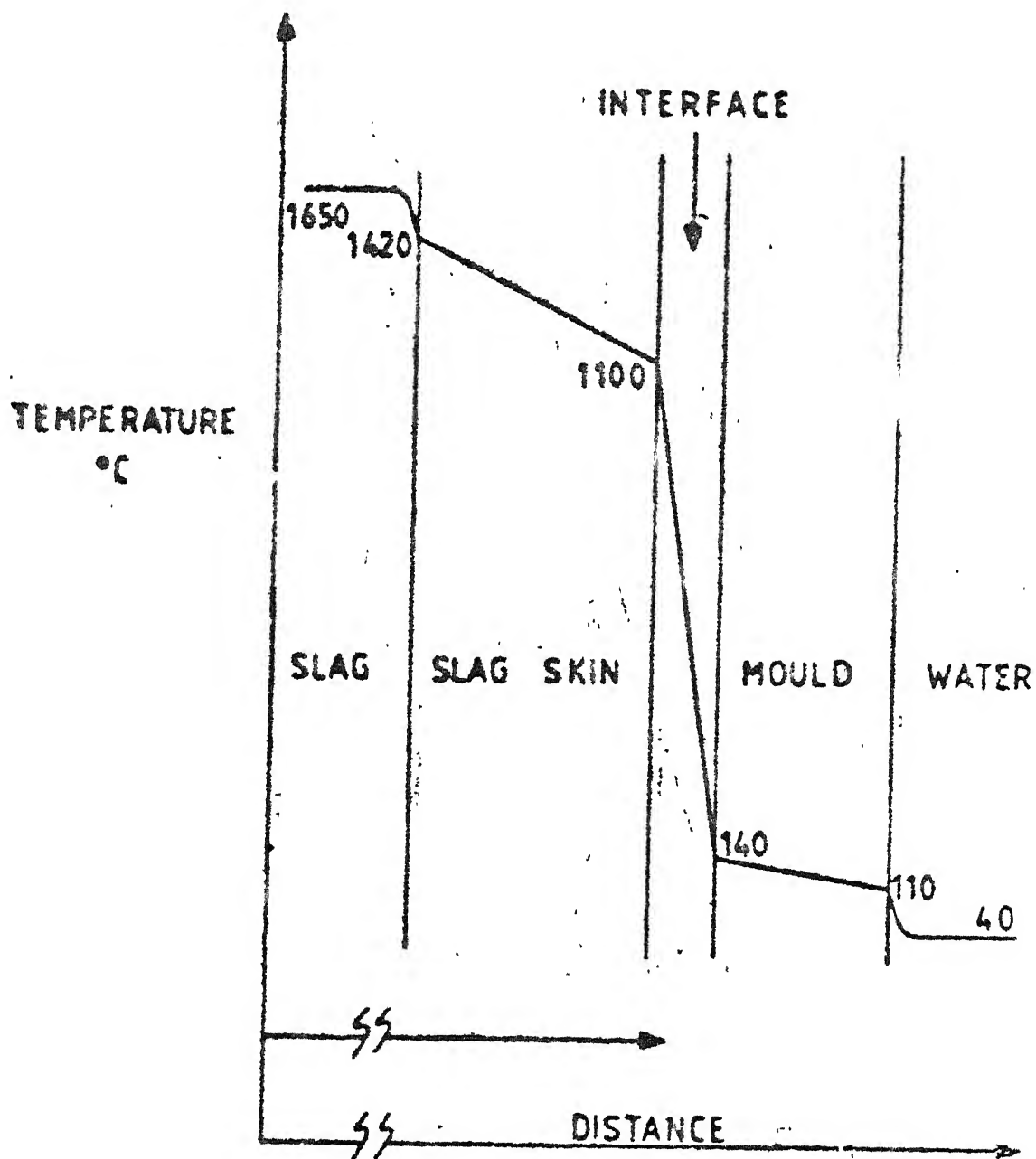
.24. Temperature gradients in slag mould interface. of ESR

CHAPTER III

PLAN OF THE PRESENT WORK

In the present work efforts have been made to study the effects of the various paths of current flow on the heat transfer patterns and mixing of the slag bath by using low melting point baths of NH_4Cl-H_2O solution and liquid $ZnCl_2$, in the double walled copper mould which acted as one electrode. The other electrode consisted of the copper tube or the manufactured lead electrode. The laboratory model studies consisted of the following :

1. Manufacturing of lead electrode.

2. Development of the technique to melt the solidified $ZnCl_2$ in the mould.

3. Modification of the existing copper mould as to provide a metal cover at the top to withstand high temperatures, cut down the heat losses and act as a guide to hold the electrodes in the vertical position.

4. Heating of the NH_4Cl-H_2O solution in the mould with and without insulation of the mould walls and the base to change the paths of current flow.

5. Heating of $ZnCl_2$ bath using copper electrodes with and without (a) Manual stirring of the bath (b) insulation

of the electrodes and the measurement of temperature at two locations of the bath corresponding to the current responses.

6. Fabrication of the arrangements to hold and lower the lead electrode at the desired speeds in the bath.

7. Heating of the $ZnCl_2$ bath using lead electrode and measurement of temperature responses at two locations, melting rates of lead and current variations.

8. Discussion of the results obtained in (4) to (7) above.

CHAPTER IV

EXPERIMENTAL

4.1 Materials Used

a) NH_4Cl : This was supplied by BDH Laboratory
Chemicals Division, Glaxco Laboratories (India) Ltd.,
Bombay which is having a minimum assay of 99.5%.

b) $ZnCl_2$: This was supplied by Thomas Baker (Chemi-
cals) Pvt Ltd., Bombay. $ZnCl_2$ supplied had a minimum assay
(ex total Zn) 97%. Physical properties and variation of proper-
ties of $ZnCl_2$ are given in Tables 4.1 and 4.2[16] respectively.

c) Lead : Lead used for the experiment was of commer-
cial purity. Physical properties of lead are given in
Table 4.1.

d) Electrode :

i) Nonconsumable : This consisted of a 4 mm OD
copper tube.

ii) Consumable : This was manufactured in the labora-
tory using lead material.

4.2 Equipments Used

a) Transformer : Power required for the process was
supplied by an oil cooled, single phase, 6.6 KVA transformer.

Table 4.1 Physical properties of Pb and $ZnCl_2$

	density gm/cm^3	sp. heat cal/gm	thermal conductivity J/sec/ cm/^{o}C	melting point ^{o}C	Boiling point ^{o}C	Heat of fusion cal/gm
$ZnCl_2$	2.9	.15	-	283	732	40.6
Pb	11.06-.0012T^{o}C	.031	346	327	1744	5.9

Table 4.2 Variation of properties with temperature $(ZnCl_2)$[16]

Temperature ^{o}C	Density gm/cc	Viscosity	Conductance
320.1	2.504	-	.0017
350	2.481	1030	.0069
400	2.459	355	.0201
450	2.454		.0482
500	2.410		.0916
550	2.388		.1573
600	2.366		.2417
650			.3464
700			.4649

It was capable of supplying a maximum current of 40 A at any fractional voltage of 250 V.

b) Mould : This was a double walled cylinder with an ID of 78 mm as given in Fig. 4.1. It was the same used by Agarwal.[17] The mould walls consisted of copper tubing while the base was made of brass material which was locally available. The cover of the mould was made of copper. The outerwalls were made of stainless steel.

c) Temperature Measuring Devices : Chromel-Alumel thermocouples were used to measure the temperatures inside the bath. A mercury thermometer was used to measure the cooling water temperature conveniently. A digital millivoltmeter was used to measure the   voltagedeveloped in the thermocouples. The thermocouples were connected to the millivoltmeter with crocodile clips through a cold junction. The thermocouples were protected from the bath by thin glass protection tubes.

d) Current and Voltage Measuring Devices : There were two ammeters, with ranges of 0-15 A and 0-100 A respectively for the measurement of current. For the measurement of low current values the first ammeter was used. A voltmeter with a range of 0-250 V was used to measure the voltage between the two electrodes.

e) Torch; LPG and Oxygen Cylinders : They were mainly used for the manufacturing of lead electrodes, by melting lead in a steel crucible.
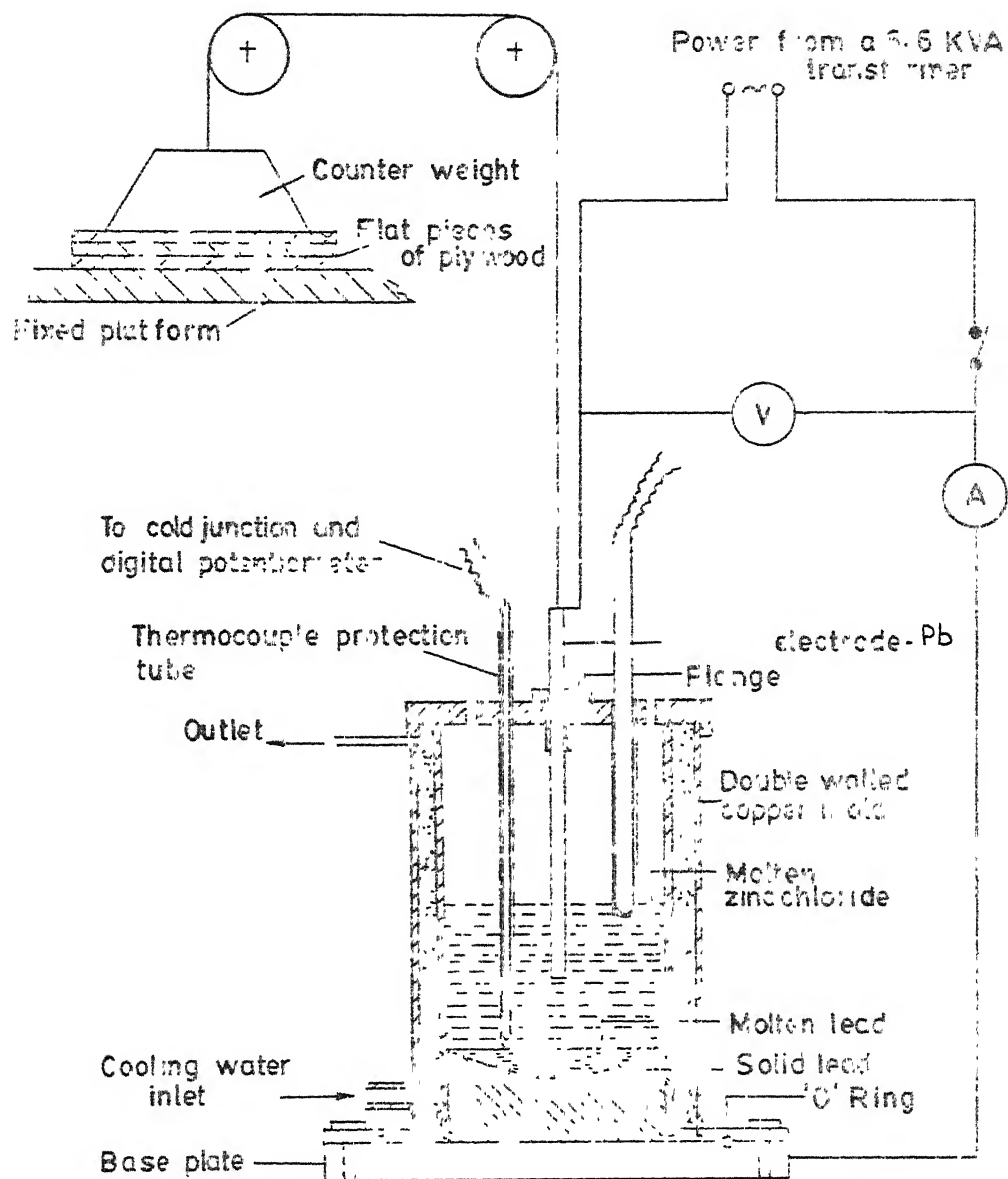
FIG. 4.1   SCHEMATIC ARRANGEMENT OF THE LABORATORY ESR UNIT

4.3 Procedure of the Experiment

a) The Electrode : A glass flange was used to insulate the electrode from the copper mould which was covered with a copper lid at the top to cut down the heat losses and fumes. The flange also acted as a guide to keep the electrode in the vertical position. The electrode was held in a desired position by using a cotton string which was supported on two pulleys. A counter weight on the other side of the string as shown in Fig. 4.1, held the electrode in a fixed position. The lowering of the electrode was done by raising the weight manually at regular intervals of time by inserting 6 mm thick flat pieces of plywood between the weight and the base. The electrode was connected to the cables for the supply of power using clips.

b) Melting of $ZnCl_2$: Initially 500 gm of the granular $ZnCl_2$, dissolved readily in 50 ml of water and the solution was found to conduct electricity satisfactorily. This could be heated by passing about 10 A of current between the electrode and the mould. As the temperature increased above $100^{\circ}C$, water started getting boiled out. The bath continued to retain its conductivity till it melted in about half an hour or so. The current was found to fall continuously till the mass melted at about $285^{\circ}C$. There was then a gradual increase in conductivity thereafter. The conductivity reached zero when the molten mass solidified.

The subsequent melting of the solidified mass inside the mould after each experiment was made possible by adding about 20 ml of water which made the top layer conductive to the flow of current. The top part then got heated to 300°C or so in 10 minutes where $ZnCl_2$ melted but the bottom of the solidified flux showed little rise in temperature. Continuous stirring and lowering of electrode thereafter helped to melt the whole mass in about one and a half hours of time. The attempts to melt the flux by directing the flame of the bunsen burner or by using graphite electrodes did not succeed. It was not possible to take the solidified flux out of the mould for remelting it outside, over the gas flame or in a furnace. The external heating of the whole mould from the bottom to melt the flux was not found practical.

c. Cooling Water : In some experiments water was passed through the annular space of the mould walls to provide cooling of the bath and to form a skin of solidified flux along the inner walls of the mould. A water tank of 30 litre capacity was kept at a height to provide the driving force for the flow of water and the efflux was collected in another reservoir below. The arrangements helped to maintain a flow rate of about 19 cc/sec throughout the experiment. The fall in level of the water in the overhead tank was made good by the addition of tap water. The temperature of the efflux was measured conveniently using a mercury thermometer.

4.3.d) Heating of Bath Using Copper Electrode (Noncorsumable):

i) NH_4Cl-H_2O System : 5-10 gms of NH_4Cl was dissolved in 1000 cc of water. This was acting as the electrolyte. The outer ends of the protection tubes of the thermocouples were adjusted to the desired positions in the bath, for measuring the temperature responses. The copper electrode was held and maintained at the desired depth of immersion in the bath and the necessary current was allowed to flow between the electrodes and the mould material by adjusting the voltage in the transformer. In some experiments the inner mould walls were insulated partially or completely using a glass tube. In some experiments the bottom base and a part of the walls were insulated   before passing the current. The current, voltage and the two temperature measurements were made at regular intervals of 30 secs or so.

ii) $ZnCl_2$ System : About 3 kg of lead was melted in a crucible and added to the double walled copper mould to act as the base. 500-1000 gms of $ZnCl_2$ was melted in the mould above the lead base in a manner described in Section IV.3.b. The ends of the protection tubes for the thermocouple were adjusted to the desired position in the bath, for measuring the temperature responses. The copper electrode that was inserted in the system to cause melting of the flux was held at a certain height in the mixture and maintained at the desired depth

of immersion in the bath. The necessary current was allowed to flow between the electrode and the mould material by adjusting the voltage in the transformer. In some experiments the slag bath was stirred vigorously to make the temperature more or less uniform with the help of a glass rod. The current, the voltage and the two temperature measurements were made at regular intervals of 30 secs or so. In some experiments when the bath was fully molten cooling water was passed in the annular space of the mould. In experiments with insulated electrodes, the copper electrode was shielded by a 6 mm ID open pyrex tube to a certain depth.

4.3.e) Heating of Bath Using Lead (consumable) Electrodes :
The procedure was similar to the one described above till the $ZnCl_2$ melted. Thereafter the copper electrode was removed and a lead electrode manufactured as explained in Section 4.3.a. was held, positioned and lowered by a mechanism described in Section 4.3.a. The two temperatures, the current and the voltage were measured. The value of the current changed rapidly during the time interval due to the consumption of the electrode. The maximum recorded value of current, recorded at the time of just lowering the electrode was noted. The length of the lead electrode as well as the weight were measured before and after each experiment.

CHAPTER V

RESULTS

The experiments carried out in the present study can be
divided into various categories depending upon the type of
the electrode used, cooling of the mould walls by passing.
water and insulation of the mould walls or the electrode.
The details of the experiments carried out and the categories
are given in Table 5.1.

W categories of experiments were conducted with 2% NH_4Cl
solution in water as the slag media and copper as the non-
consumable electrode material. In experiments W_1 and W_2 an
electrode immersion of 5 cm was used whereas in W_3 and W_4 it
was 10 cm. In WI category of experiment, the mould walls
were insulated using a glass tube to ensure the flow of
current from the tip of the electrode to the mould base. Here
also the depth of electrode immersion was varied from 5 cm
to 10 cm. W_B category of experiment was performed by insulating
the base of the mould as well as the side walls below the
electrode immersion using a glass beaker to ensure the flow of
current from the electrode surface to the mould walls for
comparison purposes. W_{AE} category of experiment was carried
out by insulating the mould base by a glass plate and the mould

walls above the electrode immersion. Current could flow from the electrode surface to the mould walls below the level of electrode immersion. The results of all these categories of experiments are given in Table 5.2.

AN category of experiments were conducted with molten $ZnCl_2$ as slag and copper electrode. Experiment AN_1 was carried out to study the thermal behaviour of the bath, i.e., the temperature gradient between the bottom layer and the top layer of the slag after the manual stirring was stopped. The temperature difference between the two layers was brought within 25 to 30 ^{o}C by manuel stirring before hand and this got increased to more than 120 ^{o}C in a time interval of less than 10 minutes. The results of these experiments are plotted in Fig. 5.1. Experiment AN_2 and AN_3 were conducted to see any changes in the temperature patterns of the bath with the lowering or switching off the voltage or the power supply to the system. The results shown in Figs 5.2 and 5.3 indicate that the bath temperature tended to become more uniform after lowering the voltage. In AC series of experiments, cooling water was passed through the annular space of the mould walls after the bath was melted as discussed in Section 4.3b. The results plotted in Figs 5.4 & 5.5 show that the bottom most layer which was already at a lower temperature than the upper most layer, solidified rapidly with passing of the cooling water and it further obstructed the flow of current from the electrode tip to the base plate. When attempts were made to increase the

power supply in order to avoid freezing of the bath, copious fumes were evolved out from the top of the bath. Experiment AC_3 was conducted to study the temperature behaviour of the slag upto the level of electrode immersion and the results in Fig. 5.6 show that there was not much difference in temperature between the uppermost layer and the layer near the tip of the electrode even without any stirring.

AI category of experiments were carried out after insulating the electrode upto the tip as to obstruct the flow of current from the electrode surface to the mould walls and allow the current to flow from the tip of the electrode to the mould base through the molten bath. In such experiments the results plotted in Fig. 5.7 and Fig. 5.8 showed that the bath temperature was more uniform w even without any stirring. In experiment AI_3, the glass tube which was used to insulate the electrode projected 1 cm beyond the electrode tip as to ensure further. the flow of current from the electrode tip to the mould base and results in Fig. 5.9 show that there was practically no difference in temperature between the topmost and the bottom most layers in such a case.

BN category of experiments were carried out using consumable lead electrodes as to simulate the condition occurring in the electro slag refining of metals. In BN_1 the feeding of the

electrode was regulated by the current which decreased as the electrode material tended to melt. As soon as the current value became less than 5A or so, the electrode was manually lowered in steps of 1.2 cm as explained in Section 4.3a. There were thus rapid fluctuations in the value of current which is plotted in Fig. 5.10, along with the measured temperature responses. Experiments BN_2 and BN_3 were performed by lowering the electrodes in steps of 6 mm at regular time intervals of 30 seconds. The current value could be measured at the time of lowering of the electrodes. The dynamic responses of the current in the short intervals of 30 sec could not be measured in such experiments; but it did fall below 5A during the time interval of the successive lowering of the electrode. The results of the temperature responses are shown in Fig. 5.11 and Fig. 5.12 respectively.

In experiments BC_1 and BC_2, cooling water was allowed to flow through the annular space of the mould walls soon after the copper electrode was replaced by the lead electrode. In experiments BC_2, the bottom most and the top most temperatures were brought closer before hand by manul stirring of the bath. The results of the temperature response measurements in these two experiments are plotted in Figs. 5.13 and 5.14 respectively.

Table 5.1

Details of experiments carried out in the present work

Electro-lyte	Cate-gory	Bath height cm.	Electrode immersion cm.	Position of thermocouples cm.		Cooling water flow cc/sec	Voltage Volts	Re-mar
				TC_1	TC_2			
1	2	3	4	5	6	7	8	9
Copper electrode, NH_4Cl-H_2O	W_1	15	5	4	10	-	20	*
	W_2	15	5	1	7	-	20	
	W_3	15	10	4	10	-	20	
	W_4	15	10	1	7	-	20	
NH_4Cl-H_2O, Cu electrode	WI_1	15	5	4	10	-	65	
	WI_2	15	5	1	7	-	65	
	WI_3	15	10	4	10	-	65	
	WI_4	15	10	1	7	-	65	
NH_4Cl-H_2O, Cu electrode	WB_1	15	5	4	10	-	20	
	WB_2	15	5	1	7	-	20	
NH_4Cl-H_2O, Cu electrode	WAE_1	15	5	4	10	-	20	
	WAE_2	15	5	1	7	-	20	
Molten $ZnCl_2$, Cu electrode	AN_1	6	2	1/2	6	-	37.5	
	AN_2	6	2	1/2	6	-	30-55	
	AN_3	6	2 1/2	1/2	6	-	0-62.5	

1	2	3	4	5	6	7	8	9
Molten $ZnCl_2$, Cu electorde	AC_1	6	2 1/2	1/2	6	18.9	24-60	
	AC_2	6	4	1/2	6	18.9	17.5-40	
	AC_3	6	2 1/2	1/2	2 1/2	18.9	30-55	
Molten $ZnCl_2$, Cu electrode	AI_1	5	3	1/2	5	18.9	30-53.5	
	AI_2	5	3	1/2	5	18.9	17.5-55	
	AI_3	5	3	1/2	5	18.9	35-67.5	
Molten $ZnCl_2$, Pb electrode	BN_1	6	1 1/2	1/2	6	-	25	
	BN_2	6	1/2	1/2	6	-	35	
	BN_3	6	1/2	1/2	6	-	35-87.5	
Molten $ZnCl_2$, Pb electrode	BC_1	5 1/2	1/2	1/2	5 1/2	18.9	35-112.5	
	BC_2	5	1/2	1/2	5	18.9	25-112.5	

Remarks

W   No insulation

WI   Side walls are insulated with a glass tube

WB   Bottom of the bath and the side walls upto the electrode immersion are insulated with a beaker of glass

WAE Bottom of the bath and the side walls above the electrode immersion are insulated by glass plate and a tube respectively

AI   Electrode insulated by shielding it in a glass tube except at the tip of the electrode

BN   The slag was melted with copper electrode and later replaced by using Pb electrodes.

AC   After melting of the slag, cooling water was passed.

BC   Slag was melted with copper electrode and later replaced by Pb electrodes and then cooling water was passed.

Table 5.2
Results of temperature and current measurements in the
various categories of experiments – NH_4Cl-H_2O system

Category	Time min	I amps	Temperature	
			TC_1 deg C	TC_2 deg C
1	2	3	4	5
W_1	1	6.7	30	21.5
	2	7.5	37	22
	4	8.6	48	29.5
	8	10.5	66	43
W_2	1	7.0	35	24
	2	7.7	42	28
	4	8.8	53	35
	8	10.6	72	52
W_3	1	11.6	35.5	24.5
	2	12.8	43	30
	3	14	50	35
	4	15.1	55	40
W_4	1	11	35.5	30.5
	2	12.1	43	37
	3	13	50	41
	5	14.7	61	56
WI_1	1	3.25	36	30
	2	3.6	46	42
	4	4.2	60	56
	8	5.6	83.5	79

1	2	3	4	5
WI_2	1	3.4	35	34
	2	3.9	45	43.5
	4	4.7	60	58.5
	8	6.0	89	88
WI_3	1	4	37	35
	2	5	46	43
	4	6.8	68	66
	8	9.5	99.25	99
WI_4	1	4.9	37.5	37
	2	5.5	48	48
	4	7.2	70	70
	7	9.5	98.5	98.5
WB_1	1	6.6	31	20
	2	7.4	37.5	21
	4	8.5	52	25
	8	10.7	68	37
WB_2	1	5.8	33.5	20.5
	2	6.4	40	23
	4	7.4	50	29
	8	9.1	65	41
WAE_1	1	7.0	30	22
	2	8.0	37	24
	4	9.4	49	30
	8	11.7	69	44

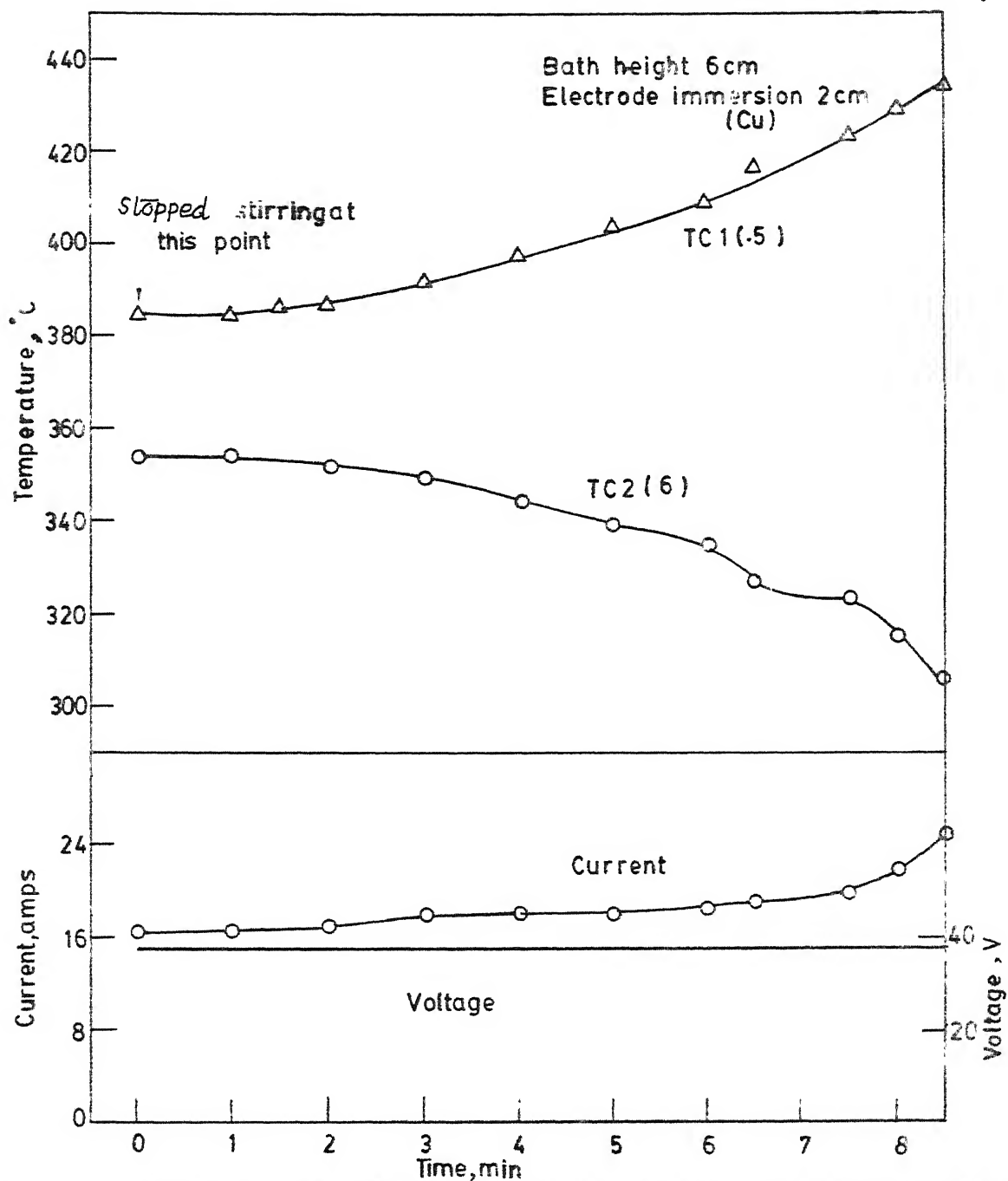| 1	2	3	4	5
WAE_2	1	7.8	36	23
	2	8.6	44	27
	4	10	56	36
	8	12.1	75	53

FIG 5.1   THE RESULTS OF THE TEMPERATURE AND CURRENT RESPONSES.
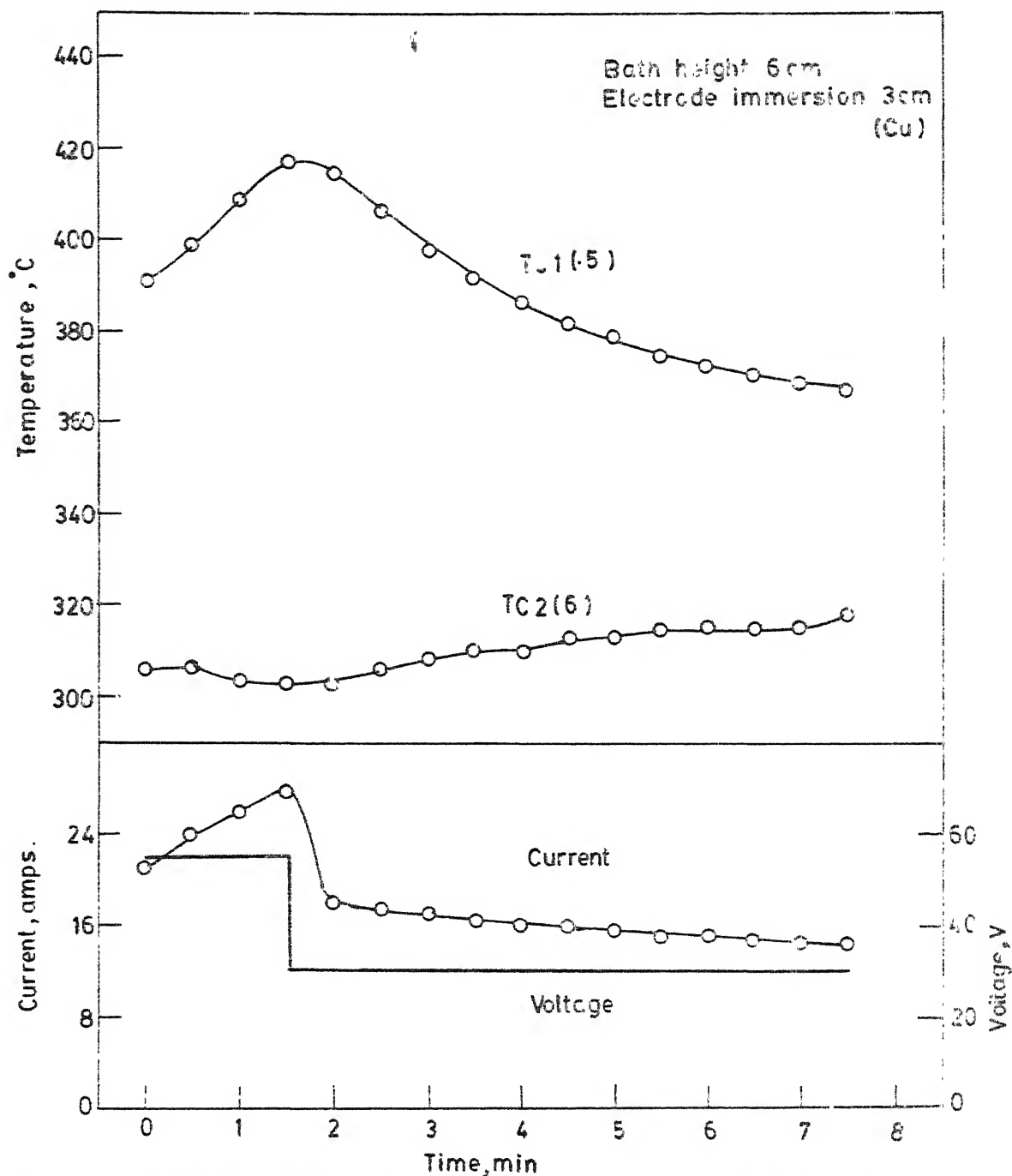EXPERIMENT AN₁

FIG 5.2   THE RESULTS OF TEMPERTURE AND CURRENT VARIATION.
EXPERIMENT AN$_2$

FIG 5.3   THE RESULTS OF THE TEMPERATURE AND CURRENT
VARIATION - EXPERIMENT AN₃

FIG. 5·4   THE RESULTS OF THE TEMPERATURE, CURRENT AND COOLING
WATER TEMPERATURE VARIATION - EXPERIMENT AC₁

Bath height 6cm
Electrode immersion
4cm (Cu)

TC 1 (·5)

TC 3 Cooling water temperature

TC 2 (6)

Current

Voltage

FIG. 5·5   THE RESULTS OF THE TEMPERATURE, CURRENT AND COOLING
WATER TEMPARATURE RESPONSES – EXPERIMENT AC₂

FIG. 5.6 THE RESULTS OF THE TEMPERATURE, CURRENT AND COOLING WATER TEMPERATURE VARIATION-EXPERIMENT AC₃

FIG. 5.7 THE RESULTS OF THE TEMPERATURE, CURRENT AND COOLING WATER TEMPERATURE – EXPERIMENT AI₁

FIG. 5·8   THE RESULTS OF THE TEMPERATURE , CURRENT AND COOLING WATER TEMPERATURE VARIATION – EXPERIMENT AI$_2$

FIG. 5·9 THE RESULTS OF THE TEMPERATURE, CURRENT AND COOLING
WATER TEMPARATURE RESPONSES - EXPERIMENT A1₃

FIG.5.10   THE RESULTS OF THE TEMPERATURE AND CURRENT RESPONSES.
EXPERIMENT BN₁

FIG. 5.11   THE RESULTS OF THE TEMPERATURE AND CURRENT
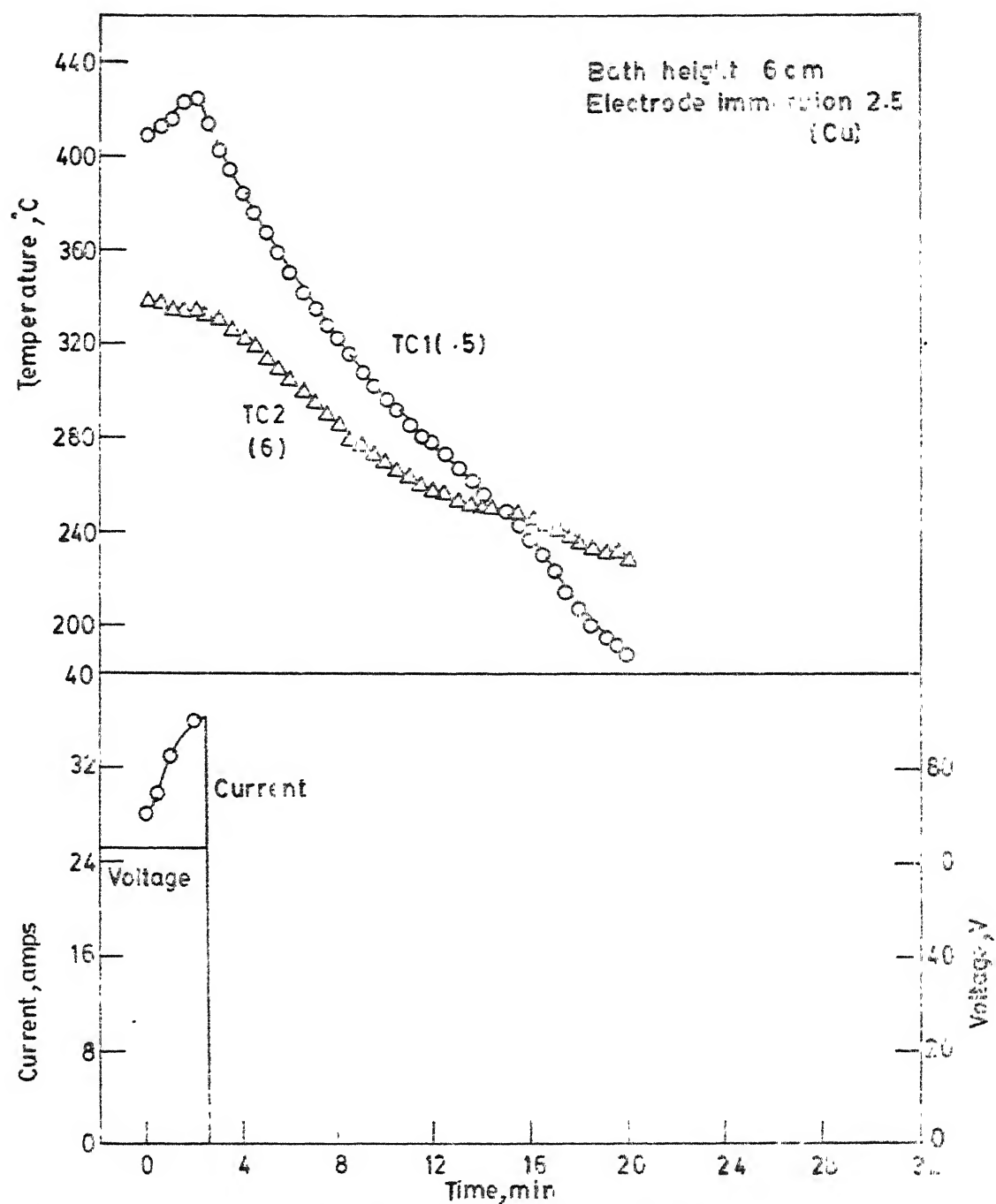RESPONSES EXPERIMENT BN_2
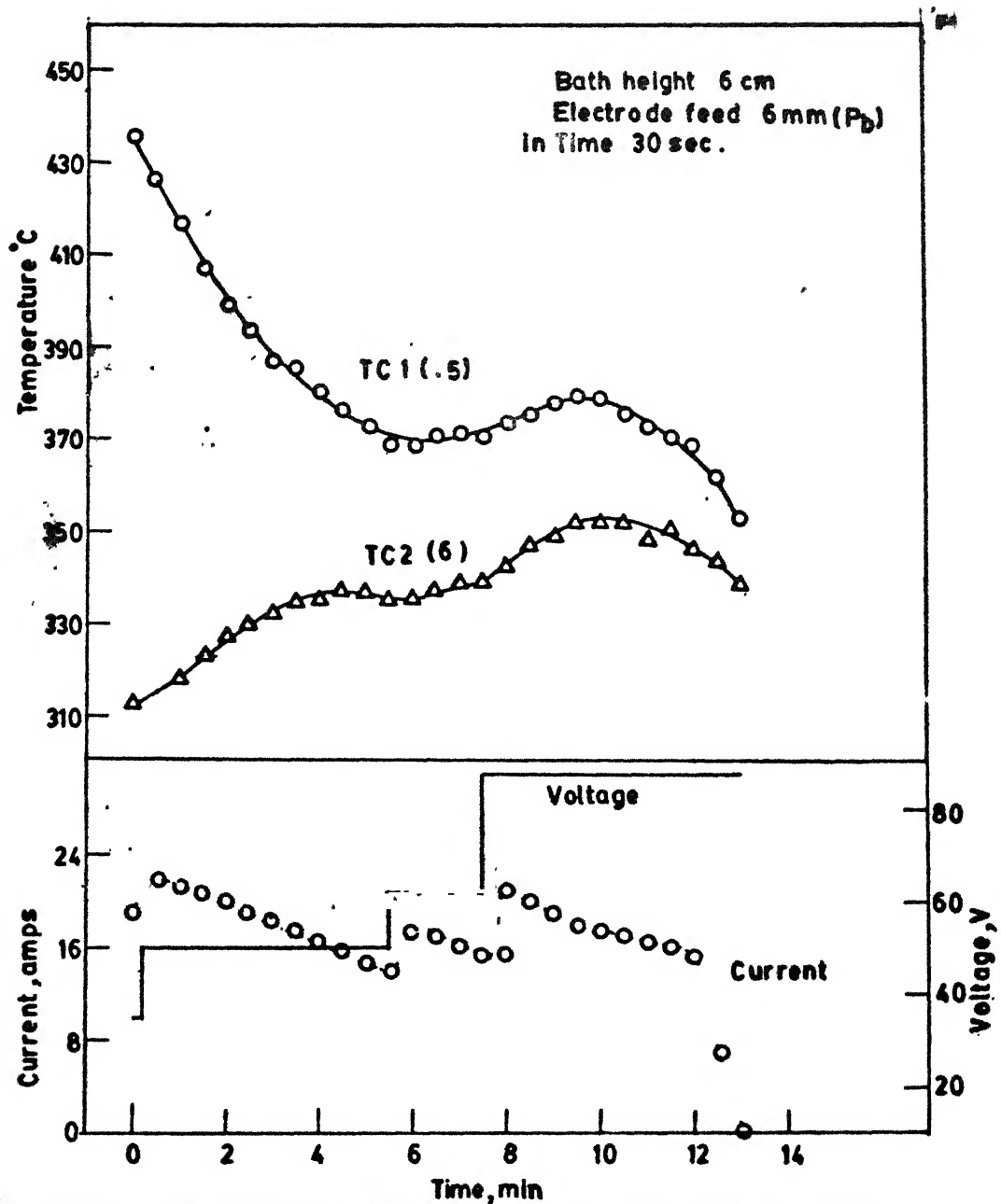
FIG. 5.12 THE RESULTS OF THE TEMPARATURE AND CURRENT
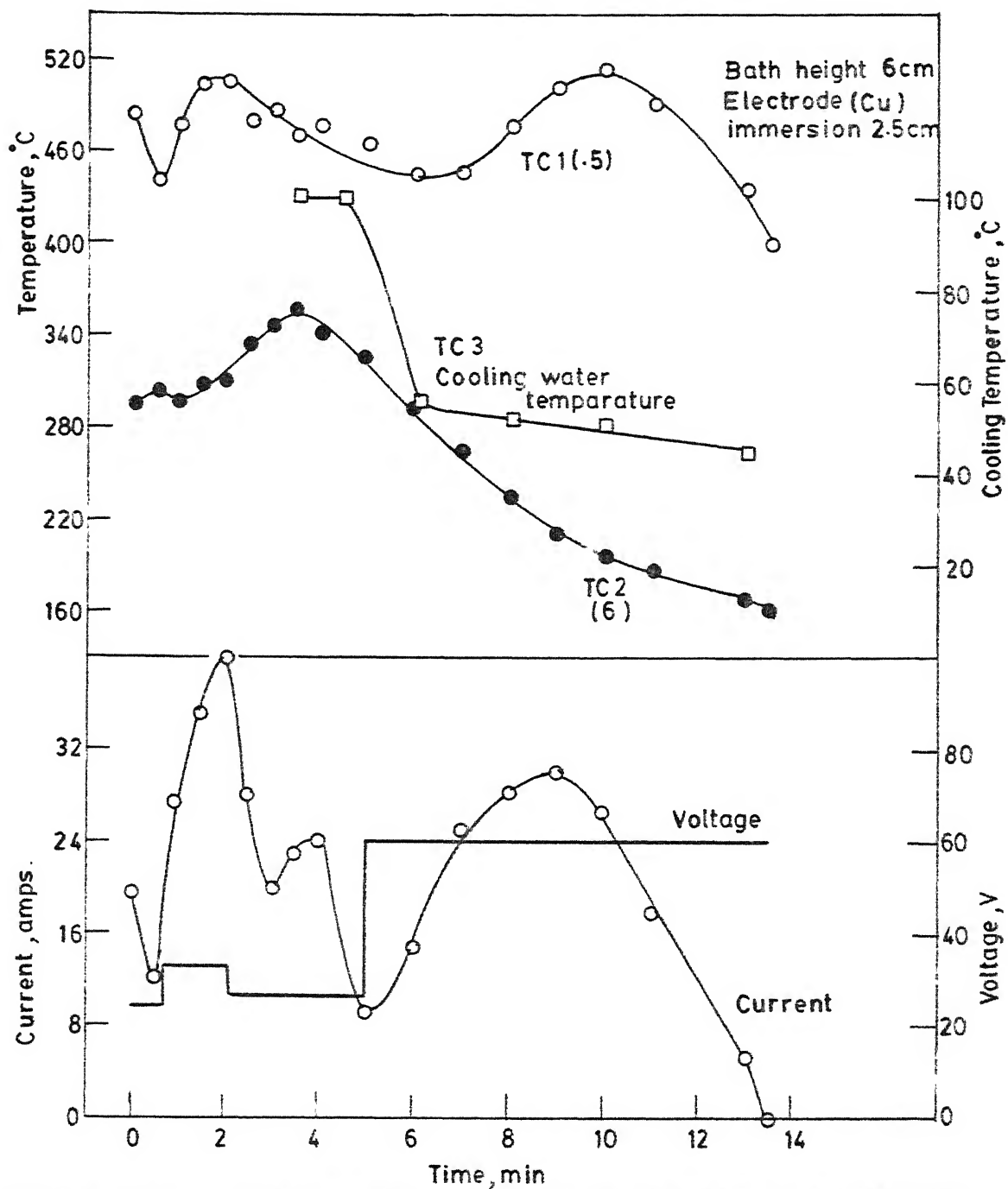RESPONSES – EXPERIMENT BN₃
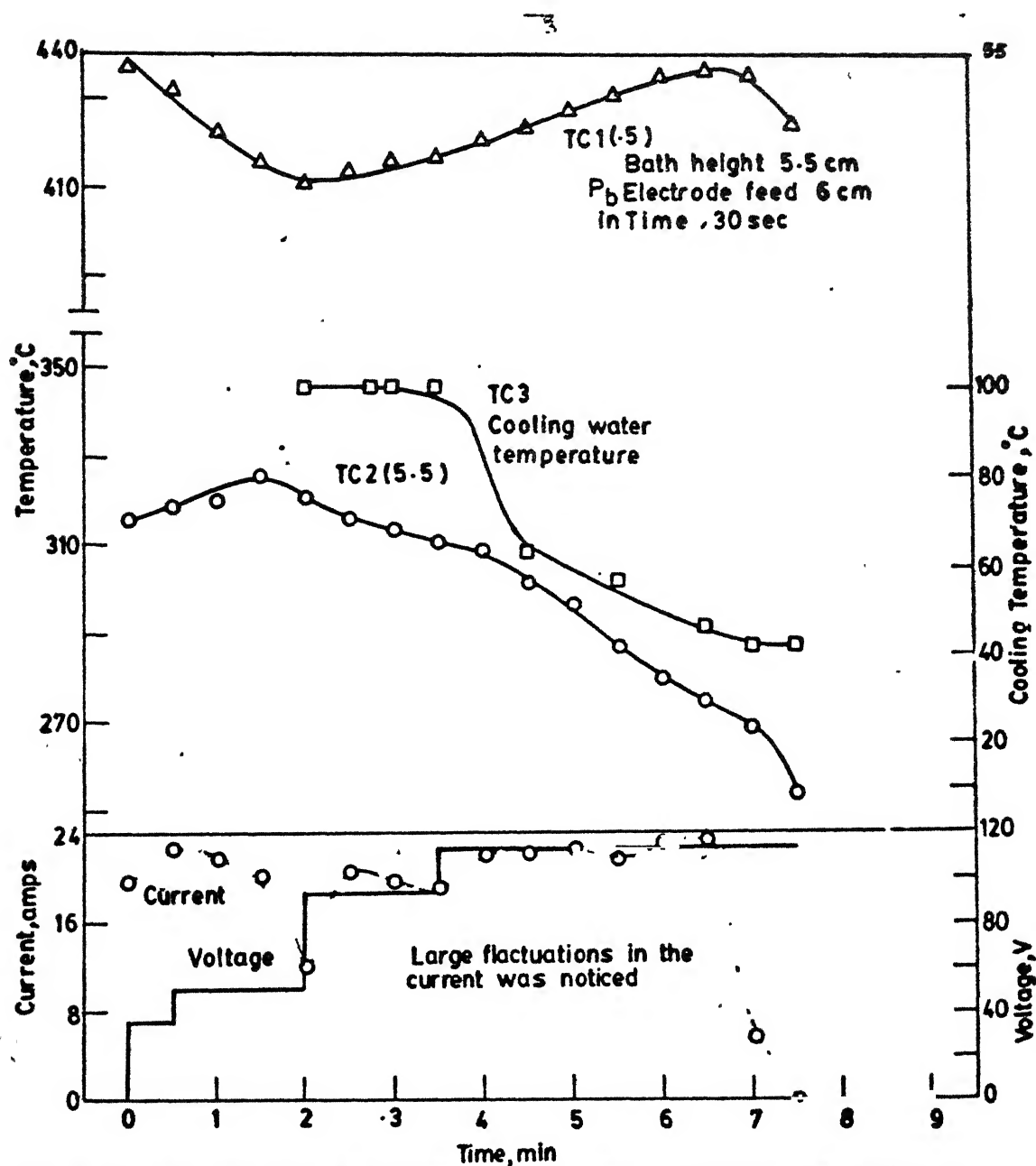
FIG. 5·13 THE RESULTS OF THE TEMPERATURE , CURRENT AND COOLING WATER TEMPERATURE VARIATION EXPERIMENT BC1
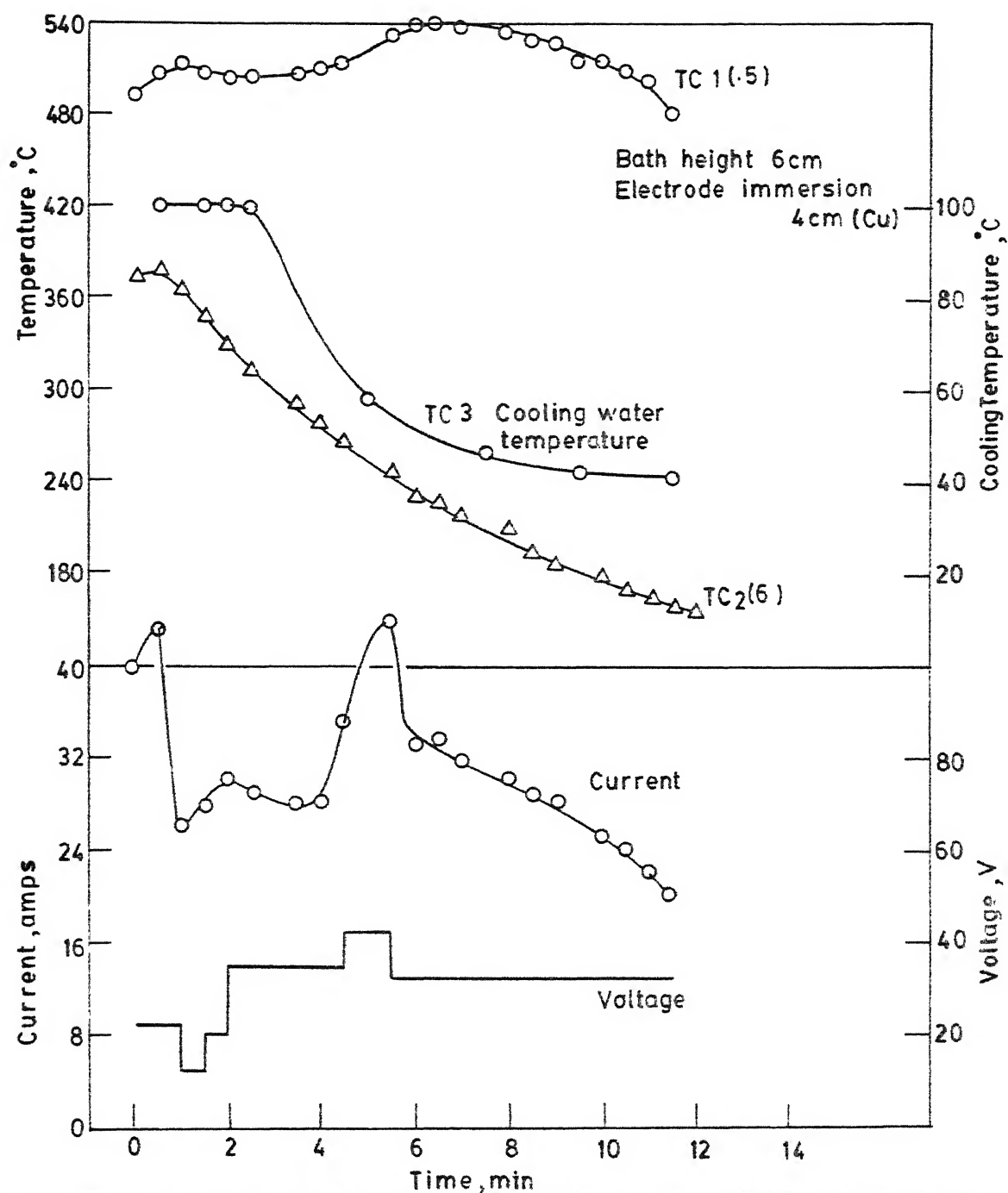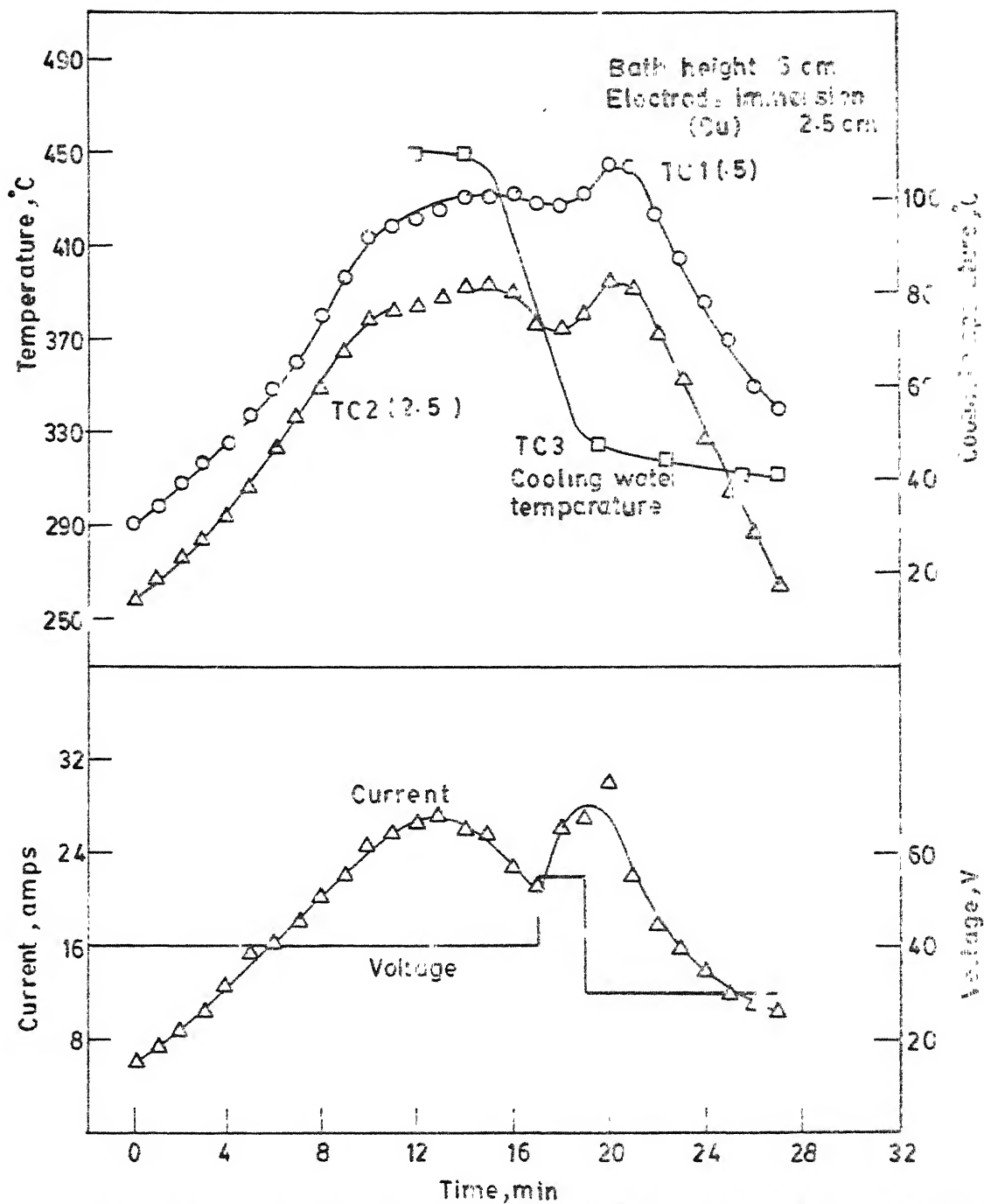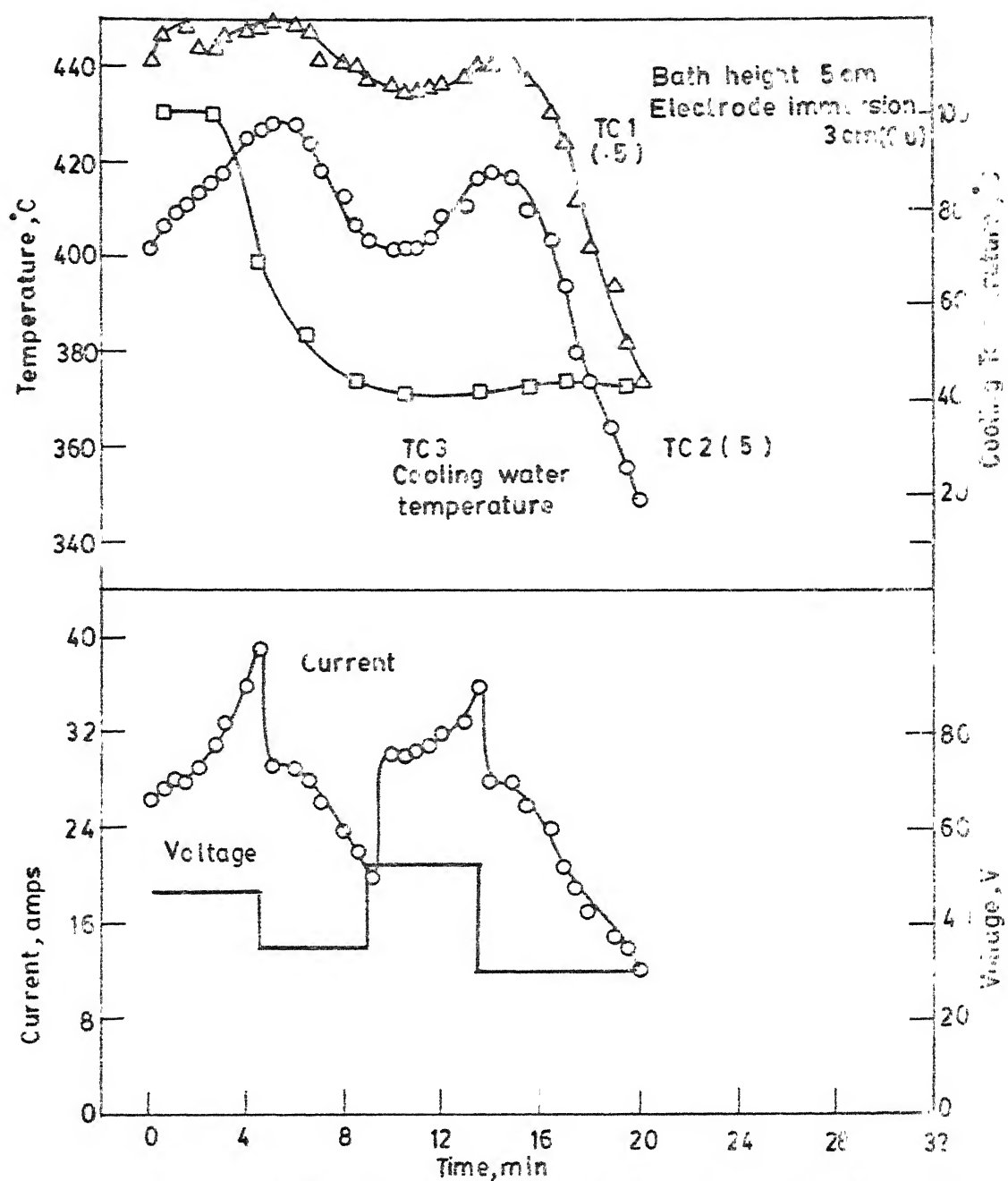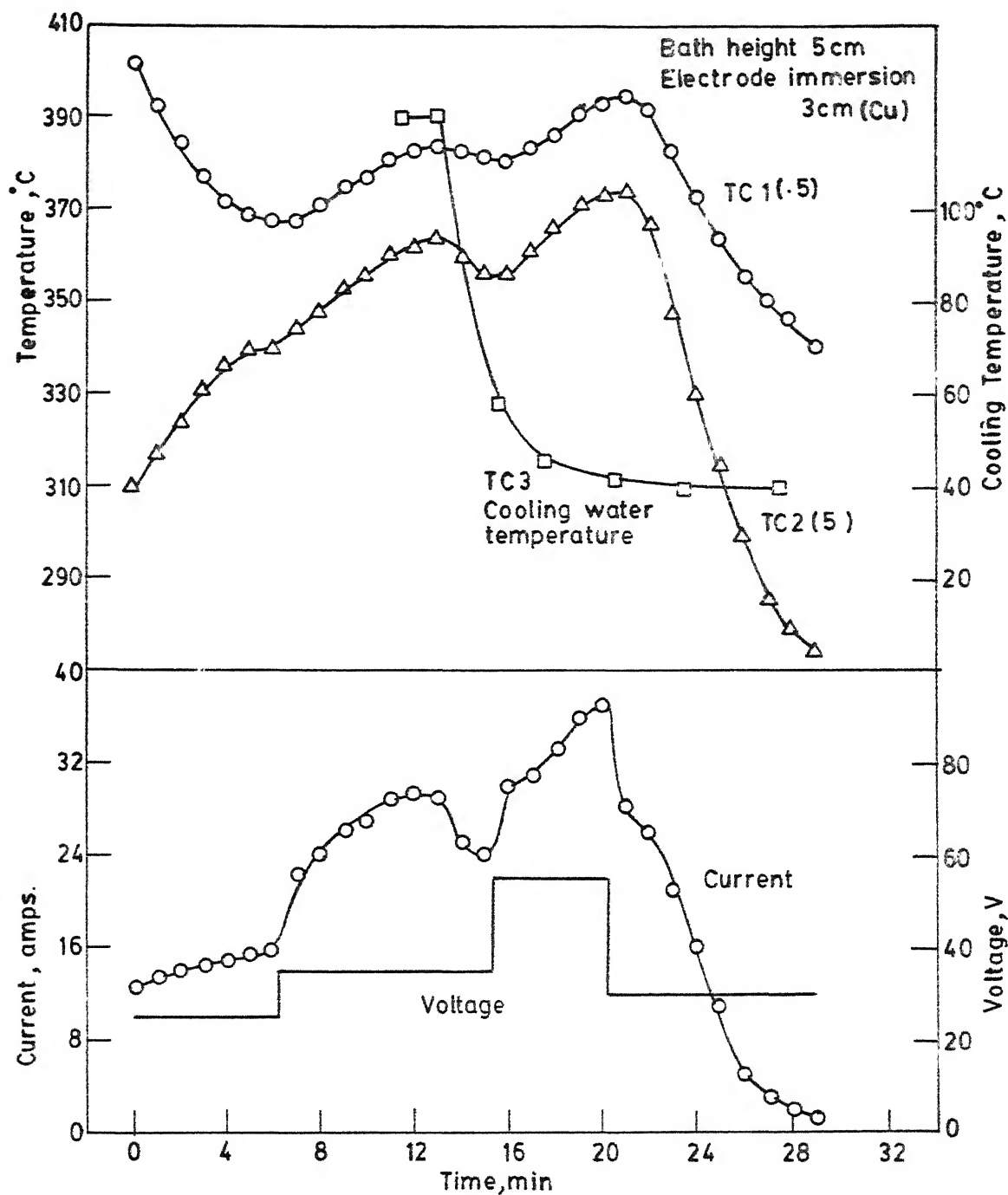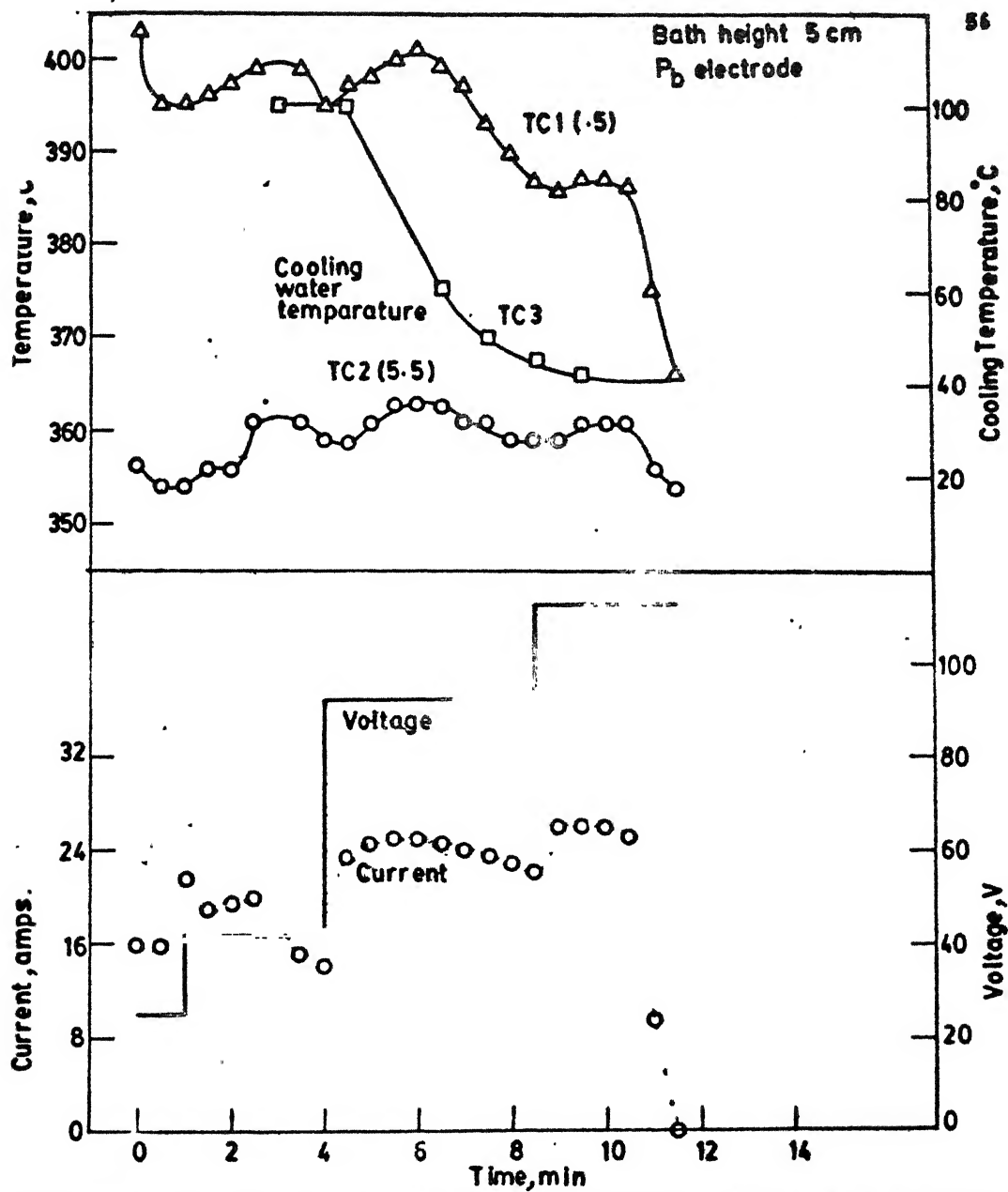
FIG.5.14   THE RESULTS OF THE TEMPERATURE, CURRENT AND COOLING
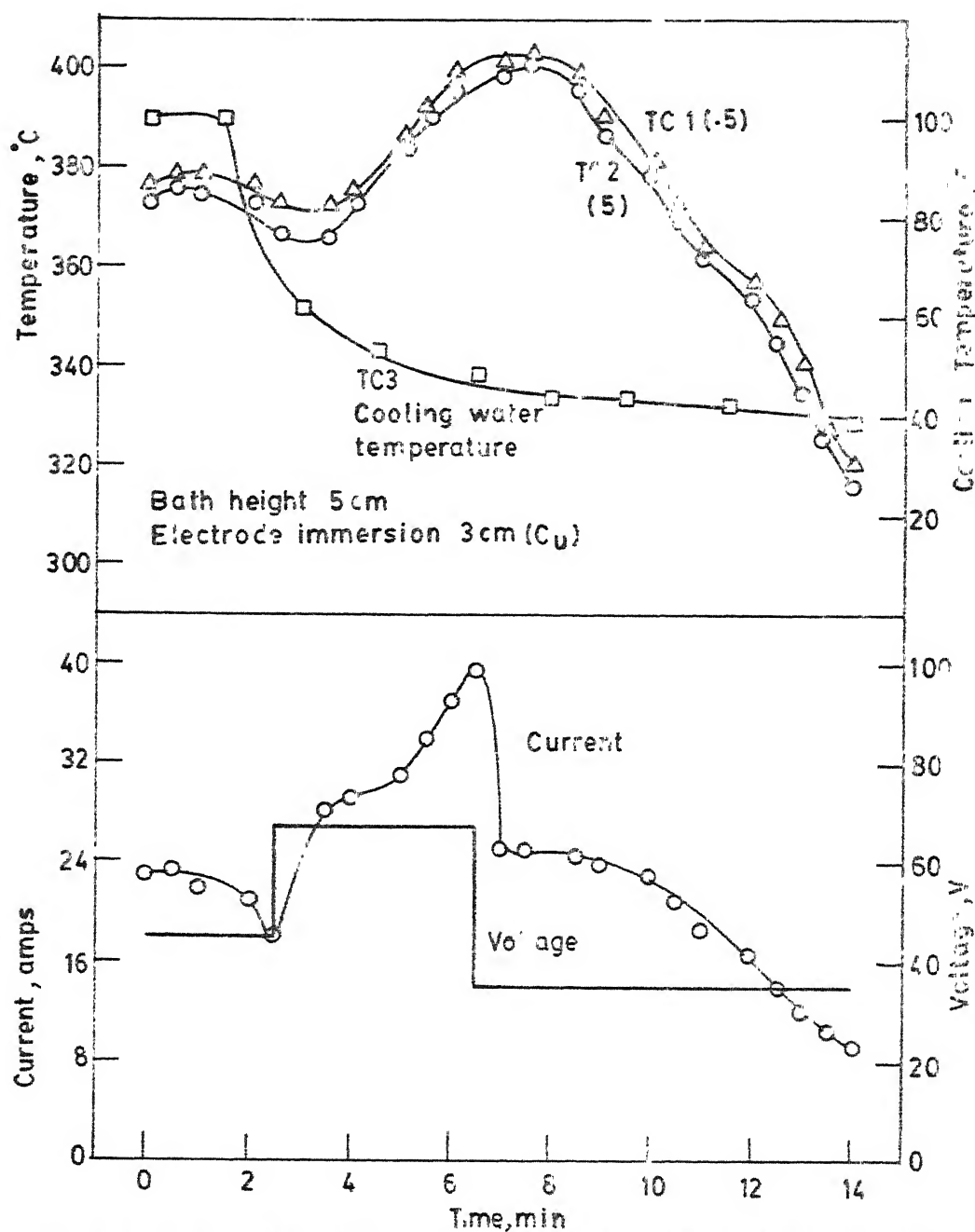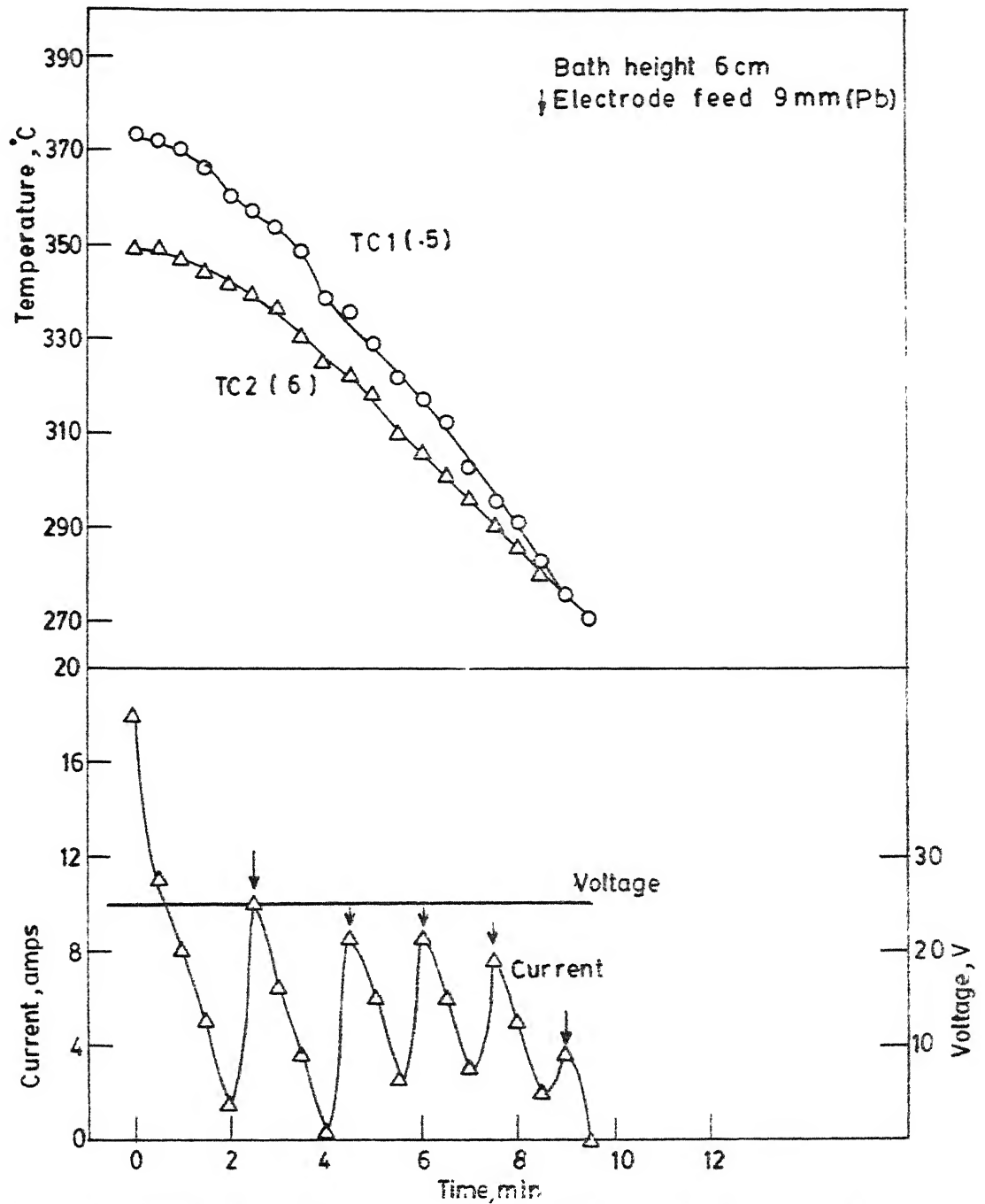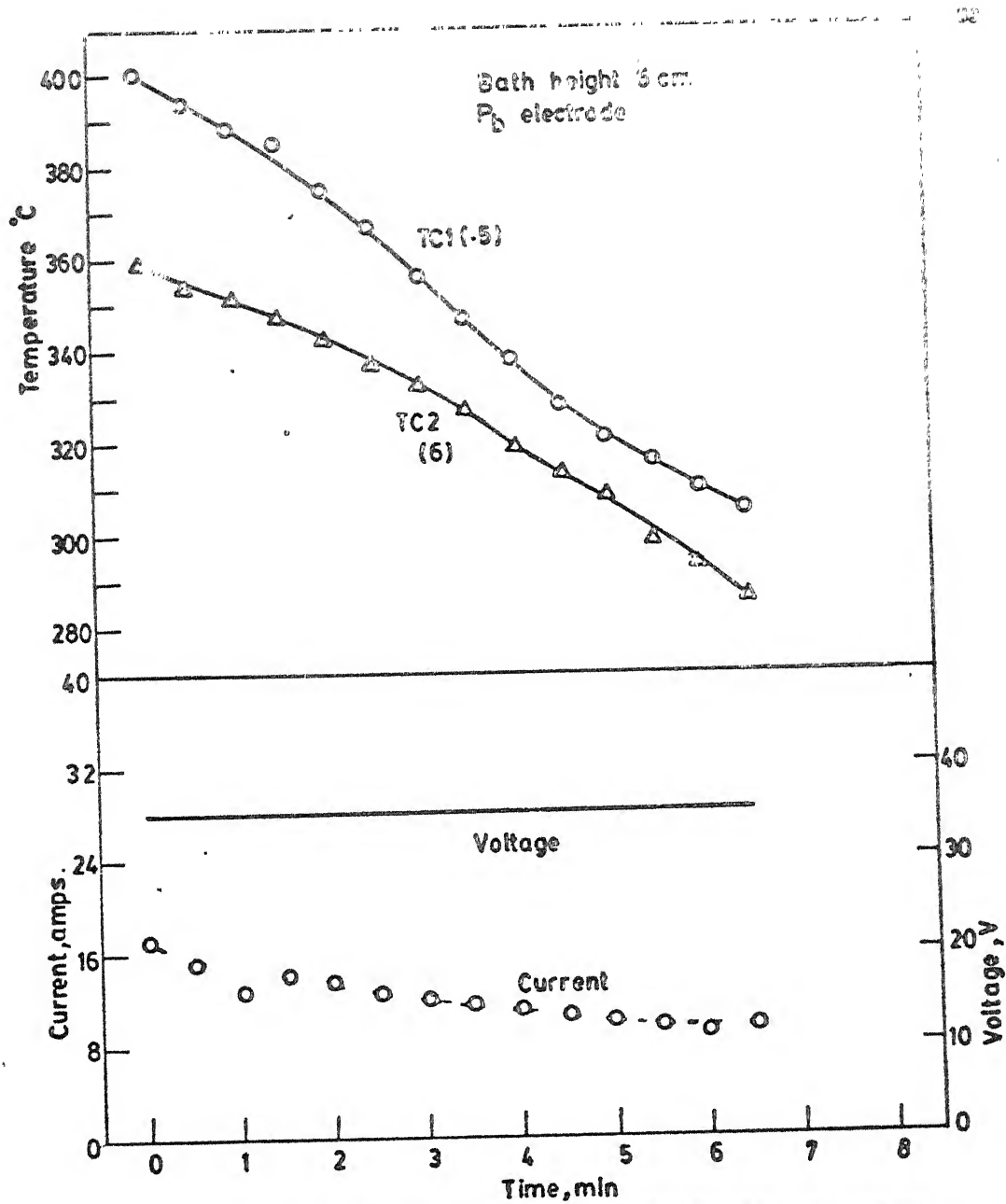WATER TEMPARATURE VARIATION – EXPERIMENT BC$_2$

CHAPTER VI

DISCUSSION

6.1 Temperature Gradients in the Bath

The results of the experiments tend to show that there is a large temperature gradient between the top layer and the bottom layer of the bath in the W, W_B, W_{AE}, AN , AC and BN categories of experiments. The results of experiments in W, WI and W_{AE} are replotted in Fig. 6.1 to show the temperature distribution in the bath after 4 minutes due to the passage of the current. The difference in temperature between the top layer and the bottom layer may be attributed to the following.

1.   Current tends to flow mainly along the shorter route between the mould walls and the electrode surface which is immersed in the bath, rather than between the electrode tip and the mould bottom. Heating is thus confined to the region upto which the electrode is dipped in the bath.

2.   As the bath in the upper region gets heated due to the current flow its electrical conductivity increases further, which in turn increases the amount of current passed and heat produced in the upper part, while the bottom part of the bath remains denser at lower temperatures. Thermal convections are not set up in the process and external stirring is required to make the temperature uniform throughout.
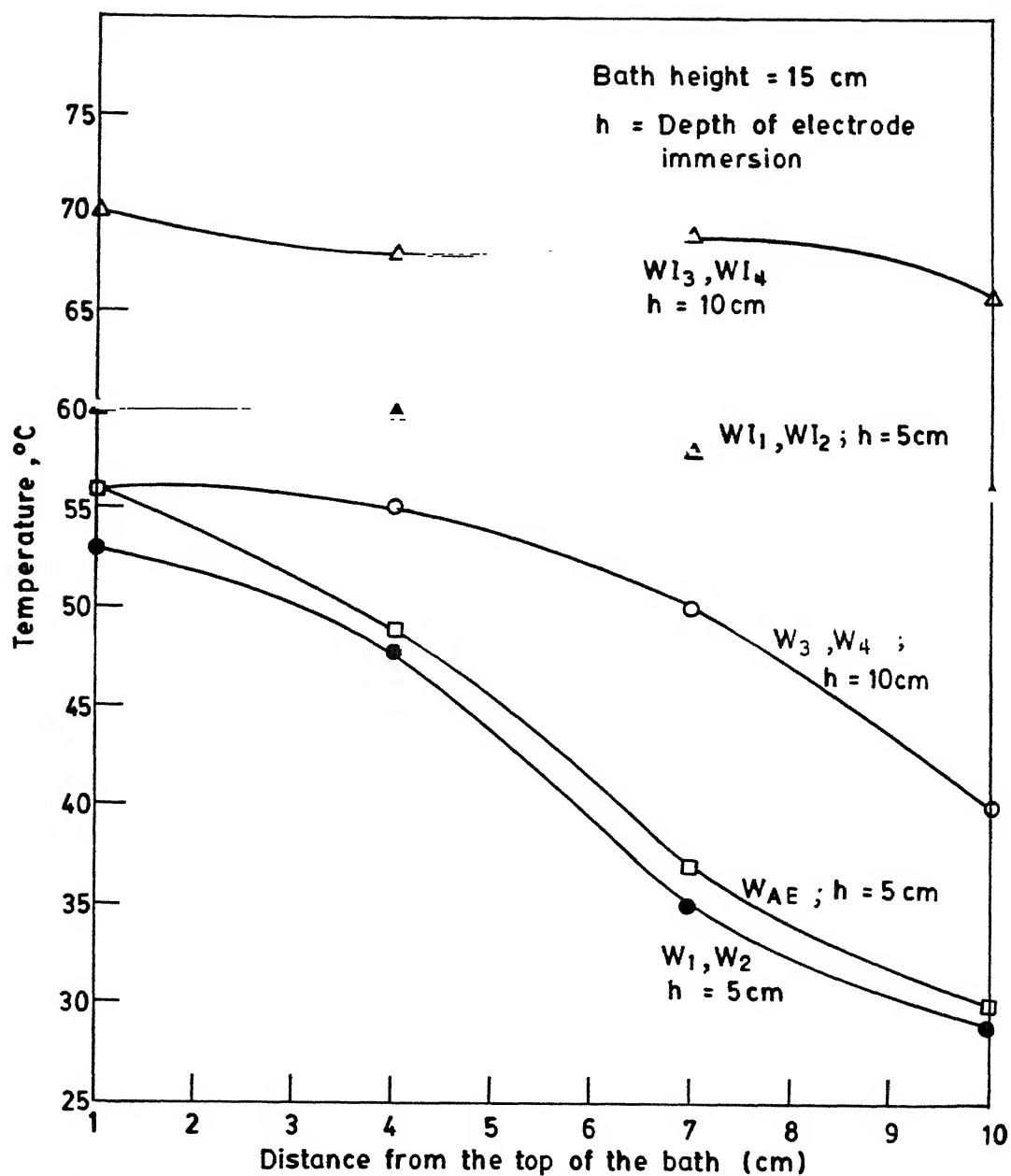
FIG. 6·1 VARIATION OF TEMPERATURE WITH DISTANCE AFTER 4 MINUTES OF TIME

If the flow of current along the shorter path between he electrode and the mould walls is obstructed either by nsulating the mould walls, (i.e., category WI) or by insulating he electrode upto the tip (i.e., category AI), the current ill tend to flow between the electrode tip and the base plate nd heating will be occurring in the portion of the bath below he electrode tip. Thermal convections are set up as the colder ass lying above the level of the electrode tip tends to move own by gravity and the hot bath moves up, making the tempera- ure of the bath more or less uniform.

The present results tend to agree well with those reported y Agarwal.[17] If the walls are not insulated there is very imited flow of current in the lower portion of the bath and the esults are not much affected whether the base plate and the ould walls below the level of the electrode immersion are nsulated or not. Thus the results of current and temperature esponses obtained in WB and W_{AE} categories are similar to hose of W categories of experiments.

.2 Model for the Electrical Resistance of the Bath

The relative flow of current in upper or the lower portions f the bath may be determined by the relative resistances of the egions which are discussed below. The probable paths of the urrent flow are schematically shown in Fig. 6.2.[17] R_a is an rc resistance due to the boiling action of water if any near :he electrode surface due to the presence of the water vapour
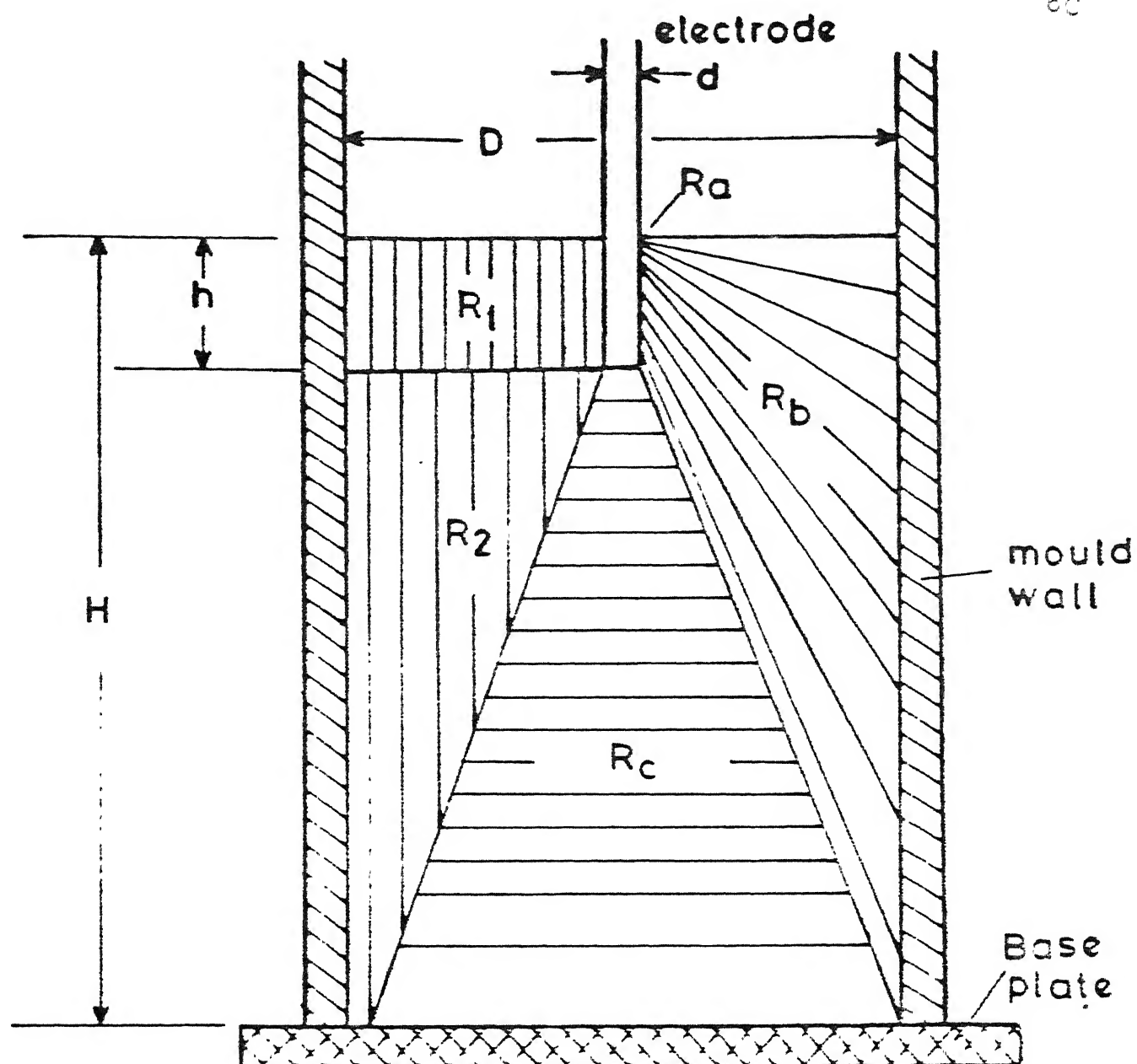
Fig. 6.2 Paths of current flow – NH_4Cl–H_2O system
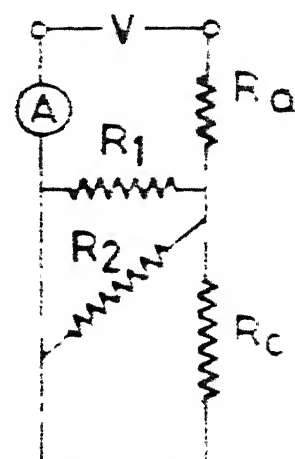
as and when temperature of the bath reaches its boiling point. R_b is the resistance of the bath bounded by the electrode and the mould walls and R_c is the resistance of the bath bounded by the electrode tip and the base. R_b and R_c may be visualised as two resistances connected in parallel, the amount of current as well as generation of heat in any resistance being inversely proportional to its value. R_b can be further thought of two resistances R_1 and R_2 in parallel, both of which will approach infinity if the walls are insulated. R_c approaches infinity when the base of the mould is insulated. For non-insulated mould R_1, R_2, R_b and R_c may be determined as follows :

$$R_1 = \int_{d/2}^{D/2} \frac{\rho\,dr}{2\pi rh} = \frac{}{2\pi h} \ln \frac{D}{d} \qquad (6.1)$$

$$R_b = \int_{d/2}^{D/2} \frac{\rho \quad dr}{2\pi r\,[h + \frac{H-h}{D-d}(2r-d)]}$$

$$= \frac{\rho(D-d)}{2\pi(hD-Hd)} \ln \frac{hD}{Hd} \qquad (6.2)$$

$$R_c = \int_{0}^{H-h} \frac{\rho\,dZ}{\pi\,[\frac{Z(D-d)}{2(H-h)} + \frac{d}{2}]^2}$$

$$= \frac{4\rho(H-h)}{\pi\,dD} \qquad (6.3)$$

where ρ is the resistivity of the slag medium

D is the inner diameter of the mould

d is the diameter of the electrode used

H is the height of the bath

h is the depth of electrode immersion

Since R_b consists of two resistances R_1 and R_2 connected in parallel

$$\frac{1}{R_1} + \frac{1}{R_2} = \frac{1}{R_b} \qquad (6.4)$$

If the bath is assumed to be uniformly mixed due to the thermal convections, R_c may be modified as follows :

$$R_c' = \frac{4 \, \rho_o (H-h)}{\pi D^2} \qquad (6.5)$$

The overall resistance of the bath is given as follows :

$$R_o = R_a + [\frac{1}{R_b} + \frac{1}{R_c}]^{-1}$$

For insulated walls, R_o may be same as R_c'. As the electrical conductance increases with increase in temperature, R_o decreases and current increases with temperature, till R_a becomes important and increases the overall resistance of the bath.

The calculated values of resistances such as R_1, R_2, R_3, R_C and R_O in terms of the parameter ρ_o by the procedure described above are given in Table 6.1. Since a new cell resistance is nothing but the ratio of the voltage applied to the current measured, it can be experimentally established **and** compared to the values *from* the above model. It may be seen that in most of the cases except for insulated walls, calculated values of ρ_o are close to each other. With the insulated walls, if the bath is assumed to be uniformly mixed and currents tends to flow over the complete cross-section of the bath, equation (6.5) may be used to determine R_C' and thus R_O. Calculations show that ρ_o came to be 40.3 for WI_1 and WI_2 and 44.84 for WI_3 and WI_4 which are very close to the values obtained for other categories of experiment.

6.3 Thermal Models

6.3.1 NH_4Cl-H_2O Bath with Insulated Walls (uniform mixing)

Heating of the bath occurs mainly below the electrode level and thermal convections are set up as the colder and denser bath at the top moves down by gravity and the hot mass at the bottom moves up. The resultant stirring of the bath makes the temperature more or less uniform as measured by the thermocouples at different levels of the bath in WI_1 to WI_4 experiments **and** plotted in Fig. 6.1. For such systems heat balance gives the following :

... of the bath assuming $R_a = 0$

Category	R_1/ρ_{-1}^o cm	R_2/ρ_{-1}^o cm	R_b/ρ_{-1}^o cm	R_c/ρ_{-1}^o cm	R_o/ρ_{-1}^o cm	$R=V/I$ Ohm	Temp. °C	Calculated ρ_o Ohm·cm
W_1 W_2	.095	.2273	.067	4.06	.0659	3.33	21	48.26
W_3 W_4	.0474	.3687	.042	2.03	.04115	2.04	21	48.57
WI_1 WI_2	∞	∞	∞	4.06	4.06	8.34	21	1.7
WI_3 WI_4	∞	∞	∞	2.03	2.03	4.645	21	2.24
W_B	.095	∞	.095	∞	.095	4.44	21	46.74
W_{AE}	∞	.067	.067	∞	.067	2.99	21	44.63
MN_1	.2464	.5221	.1674	1.624	.11518	2.083	404	13.72
AC_1	.1894	.664	.1446	1.421	.133	1.98	442	14.89
AI_1	∞	∞	∞	.812	.1162	3.75	353	32.27

$$[WC_p] \frac{dT}{dt} = VI - Q_L \qquad\qquad (6.6)$$

where W is the weight of the bath

C_p is the specific heat of the bath fluid

ρ is the density of the bath fluid

I is the measured value of current and

Q_L is the heat losses to the mould walls, base plate and

surroundings.

Both C_p and ρ are assumed to remain constant with temperature.

The calculated and the measured value of rise in temperature with time for these experiments are summarised in Table 6.2. The 10-20% discrepancies between the observed and the calculated values of rates of rise in temperature of the bath is attributed to the following.

A certain amount of heat is lost to the base plate, mould and surroundings. All these heat losses were assumed to be negligible in calculating the theoretical values of dT/dt. The discrepancy between the estimated values and the measured values tend to increase with the increase in temperature as heat losses tend to increase with temperature. The exact heat transfer model includes the estimation of heat losses through the mould walls and the base plate is very complex and beyond the scope of the present investigation.

Table 6.2   Comparison of the theoretical and the expreimental values
of dT/dt (insulated walls)

Experiment	WI$_1$			WI$_3$		
Time Minutes	1	4	8	1	4	8
Voltage Volts	20	20	20	20	20	20
Current Amps	3.1	3.6	4.2	3.75	5.3	7.05
Thermocouple position from top of the bath cm	4	4	4	1	1	1
Temp ^{o}C	31.5	45.5	59.5	32	48	69
Theoretical dT/dt	.001	.089	.09	.093	.113	.151
Experimental dT/dt	.076	.078	.0583	.082	.0875	.09
% discrepancy	6.2	12.36	35.22	11.83	22.6	40.4

6.3.2 NH_4Cl-H_2O Bath with Noninsulated Walls

In such experiments the value of the resistance R_1 computed by using equation (6.1) is much less than the corresponding values of R_2 and R_c. For example, R_1 is only 13% of R_2 and 2.3% of R_c in W_3 and W_4 categories of experiments. If I is the total current that is measured, current I_1 passing through the resistance R_1 of the bath may be determined as follows :

$$I_1 = \frac{\frac{1}{R_1}}{\frac{1}{R_b} + \frac{1}{R_c}} I \qquad (6.7)$$

A part of the heat produced in the bath due to the flow of current is lost by conduction along the mould walls and the electrode material and a part may be lost by convection to the surroundings. Heat balance in the upper part of the bath upto which the electrode is dipped gives the following equation :

$$\frac{\pi}{4} D^2 h \rho C_p \frac{dT}{dt} = \frac{VI_1}{4.2} - Q_L \qquad (6.8)$$

where   D is the diameter of the bath

h is the depth of electrode immersion

C_p is the specific heat of the bath fluid

V is the voltage applied

and Q_L is the amount of heat lost.

The calculated and the observed values of dT/dt are compared in Table 6.3. Here the discrepancy is around 20% initially and it increases with increase in temperature owing to the omission of heat losses from the calculations. Compared with the results obtained in the case of the insulated walls, the discrepancies are much higher due to higher heat losses through the mould walls when they are not insulated by inserting a glass tube.

6.3.3 $ZnCl_2$ System with Insulated Electrodes

In AI category of experiments using $ZnCl_2$ system the resistance R_1 has been made very large by insulating the electrodes rather than the mould walls. As a result of this, current tends to flow between the electrode and the bottom. As the resistance decreases due to the rise in temperature of the bath, current increases, which in turn increases the rate of heating. Thermal convections are set up as explained in Section 6.1 and the measured temperature at the top and the bottom are nearly the same. (see Figs. 5.7, 5.8 and 5.9). Here the cooling losses are large due to flow of water. A simple heat balance gives the following :

$$W_o \, C_{p_o} \frac{dT}{dt} = VI - Q_L \qquad\qquad (6.9)$$

where $Q_L = FC_p (\Delta T)\rho + Q_L'$

Table 6.3 Comparison of theoretical and experimental values of dT/dt
(non insulated walls)

Category	W_1			W_3		
Time (min)	1	4	8	1	4	8
Voltage (Volts)	20	20	20	20	20	20
Current I amps	6.5	7.7	8.8	10.2	12.1	13.85
Thermocouple position from the top of the bath (cm)	4	4	4	1	1	1
Temperature °C	28	39	43	30	43	55
Current I_1 amps	4.51	5.34	6.11	8.85	10.5	12.02
Theoretical dT/dt	.089	.1055	.1208	.088	.1033	.1189
Experimental dT/dt	.067	.081	.04	.083	.067	.05
% discrepancy	24.7	23.22	67	5.7	35.14	57.95

W_o is the weight of the bath

CP_o is the specific heat of the slag (assumed to be constant with temperature)

Q_L is the total heat lost

Q_L' is the heat lost by convection to the surroundings

F is the volume rate of flow of cooling water

C_p is the specific heat of cooling water

and ΔT is the rise in temperature of the cooling water flowing in the annular space of the mould wall from the bottom to the top.

In those experiments in which the total heat lost Q_L is less than that of the input power, temperature of the bath will increase with time, and vice versa.

There may be a temperature gradient between the centre and walls due to the flow of cooling water; but they were not measured. In some cases where the temperature of the bath remains almost steady, Q_L will be same as the value of energy being supplied by the input power. The results of the calculations to show the heat balances and estimated rise in temperature of the bath are given in Table 6.4.

In AC type experiments, the large temperature gradient exists and heat analysis is very complex. Heating is confined to the region upto the depth of electrode immersion.

Table 6.4   Heat balance ($ZnCl_2$ system)

Category	Inlet temp. °C	Outlet temp. °C	Current Amp	Voltage V	Energy input/ sec Cal/sec	Energy lost in cooling water/ sec. Cal/sec	Calculated dT/dt
AI_1	30	44	26	35	910	1111	-1.91
		42	32	52.5	1680	953	6.92
		43	28	30	840	1032	1.83
AI_2	31	53	29	67.5	1958	1747	2.01
		48	37	67.5	2498	1429	10.2
		44	25	67.5	875	1111	-2.25
		43	24.5	67.5	857.5	1032	- 1.66
AI_3	30	58	24	35	1200	2143	8.98
		46	33	55	2475	1350	10.7
		42	38	55	1900	1032	8.27
		40	21	30	630	873	·-2.314

The rise in temperature of the cooling water may be described by the following equation

$$FC_p \Delta T = \lambda (T_b - T_w) \pi (D + 2\delta) H \qquad (6.10)$$

where δ is the thickness of the mould wall

and λ is the heat transfer coefficient

Table 6.5 summarises the results of the calculations to determine the values of heat transfer coefficients for the experimental data and the calculated values are lying in the range of 0.015 to 0.020 cal/cm^2 sec^{o}C. In most of the cases these values lie within the reported range of values for the forced convection. The calculations for finding out the value of heat transfer coefficient were not made in the case of AC category of experiments since there was a large temperature difference between the different layers of the $ZnCl_2$ bath.

6.4 Mixing Phenomena with Consumable Lead Electrodes

The lead electrode could be lowered in steps of 6 mm at regular time intervals of 30 seconds. During this interval, the electrode melts and is collected at the bottom. The depth of the electrode immersion as well as the amount of current passed decreases rapidly with the consumption of the electrode material. This leads to the lowering of the heat being generated in the bath and consequently the temperature of the bath decreases with

Table 6.5 Calculated values of heat transfer coefficient

Height of the bath = 5 cm
Flow rate of water = 18.9 cc/sec
Diameter of mould = 78.4 mm

Category	Energy lost in cooling water per/sec Cal/sec	Bath temp. $T_{bath}°C$	Cooling water temp. T_w °C	$h = \dfrac{FC_p \triangle T}{\pi DH(T_{bath}-T_w)}$ cal/cm^2 sec °C
AI_1	.1111	418	44	.016
	953	409	42	.014
	1032	418	43	.0148
AI_2	1747	375	53	.029
	1429	399	48	.022
	1111	403	44	.0167
	1032	391	43	.016
AI_3	2143	432	58	.031
	1350	423	46	.0193
	1032	369	42	.017
	873	341	40	.0156

time, thereby increasing the resistance of the bath further.
This is very clear from the results of the experiments BN_1 and
BN_2 which are shown in Figs. 5.10 and 5.11 respectively. In
one experiment (BN_1), the electrode was lowered in steps of
1.2 mm at the time intervals of 60 to 90 seconds. The results
given in Fig. 5.10 did show that the current decreased rapidly
with time with the melting of the electrode material. This
made it necessary to increase the voltage during the experiments
in order to keep the bath at a near constant temperature. As
the colder electrode is lowered, it may set up its own thermal
convections as suggested by Campbell[1]. Results of experiment
BN_3 show that the two temperatures at the top most and the
bottom most layer try to become closer, owing to the melting
of the lead electrode and lowering of the same.

With water cooling the results are influenced by the fact
whether the skin is formed first or the bottom layer is solidified
in the mould. If there is a large temperature gradient between
the top and the bottom layers, the molten flux tends to solidify at
the base with the flow of cooling water through the annular space
of the mould walls. The flow of current is then confined to
the upper and hotter bath between the mould walls and the electrode
which delays the formation of the slag skin adjacent to the mould
walls and the current continues to flow between the electrode and
the walls. Thus the top most layer temperature either increases

or remains almost steady for some time whereas the temperature at the bottom most layer keeps on decreasing. As and when the slag skin is formed to obstruct the flow of any current, the temperature of the bath decreases rapidly with the continued flow the cooling water. If on the other hand the bath temperature is made more or less uniform before hand by external stirring of the system, the bottom layer does not freeze rapidly on passing the cooling water. The latent heat given out by the solidification of the molten lead may help to keep the bottom-most layer in the molten form for quite some time. During this time, a skin of solidified flux may be formed all the along the walls of the mould and the current flows from the tip of the electrode to the base. This along with the motion caused by the falling droplets help to keep the bath at uniform temperature from top to bottom.

CHAPTER VII

SUMMARY AND CONCLUSIONS

The electro slag refining is an important process of refining the ferrous and nonferrous metals as to enhance their chemical and mechanical properties to meet the stringent requirements in the space, air, submarines, nuclear energy and defence applications. In the process, the liquid slag between the material to be refined and the ingot acts as the refining agent as well as the source of heat generation due to the passage of current. One dimensional heat flow conditions can describe the temperature profiles of the electrode that is dipped in the molten slag. Heat flow condition in the metal pool and the slag bath are very complex in nature due to the continuous removal of heat by passing cooling water through the annular space of the double walled copper mould, for the formation of the slag crust and the air gap between the molten slag and the mould wall, and generation of heat in the slag. Both thermal convertional and electromagnetic forces may cause stirring of the bath. The major source of heat to the metal pool is via the transfer of the superheated metal droplets from the tip of the electrode to the pool.

In the present work the technique of the measurement of the temperature responses at two location of the bath along with

the current responses has been used to determine the extent of stirring of the bath as a function of the operating parameters such as the insulation of the mould walls, the insulation of the electrode, the power supplied, the type of the electrode used etc. The experiments have been performed using a solution of NH_4Cl in H_2O in the temperature range of 25-100°C and using molten $ZnCl_2$ in the temperature range of 200-500°C. The important findings of the investigation are given below.

1. The current tends to flow more along the shorter path between the mould walls and the electrode part which is immersed in the bath rather than between the electrode and the base when the mould wall as well as the electrode is not insulated.

2. As the bath gets heated due to the flow of current in the upper portion there is a temperature gradient between the topmost and the bottommost layer. This increases the conductivity of the bath in the upper region which in turn increases the amount of the current passed and the heating of the bath in the upper parts.

3. If the mould walls are insulated, current tends to flow from the electrode to the base; heating occurs in the lower parts of the bath and it sets up the thermal conventions resulting in uniform heating of the whole bath.

4. The results were similar if the electrode instead of the mould walls are insulated, except that the cooling of the mould walls are not small.

5. With the $ZnCl_2$ system, due to the temperature gradient, freezing of the bath at the bottom occurs, making the flow of current impossible between the mould base as cooling water is allowed to pass. As a result of this, no skin is formed in the upper part.

6. If the bath is stirred before passing cooling water, it was possible to form a skin all along the walls and the bottom layer did not freeze immediately, which helped the conduction of electricity from the tip of the electrode to the base of the mould. These are the conditions required for the electro slag refining process.

7. The temperature gradient is relatively small with the use of lead electrodes, probably due to the mixing caused by the thermal convection produced by the cold lead electrode that is lowered in the bath and also due to large fluctuations in the current flow.

CHAPTER VIII

RECOMMENDATION FOR FURTHER WORK

Melting of $ZnCl_2$ inside the mould created a lot of problems for the experiment, when it solidified inside the mould; it is not possible to take it out and melt it outside in a furnace or by other means. A torch may be designed which can direct the flame on the solidified mass for its melting before passing the current.

Another area where improvements are needed is the mechanism for uniform feeding of the electrode which could not be tried in the present work due to the lack of facilities such as Low RPM motor, gears, rack and pinion etc. This will reduce the fluctuations in the current and power supply to the bath and will enable the study of the effect of liquid metal droplets (falling from the electrode tip to the pool below) on the electrical conductivity of the bath. The dynamic responses can be suitably measured using an oscilloscope.

For studies above $500^{o}C$, i.e. melting of aluminium, brass and copper electrodes, more stable fluxes such as LiCl-KCl-NaCl

may be used and for melting of iron and steel electrodes, $CaO-Al_2O_5-CaF_2$ type fluxes are recommended. These fluxes must be melted in a separate unit and need be recovered carefully to some extent from the mould by removing the base plate and the solidified ingot in the mould, otherwise fresh quantity of slag may be made and used everytime the experiment is performed. The newly procured 25 KVA transformer may be used to obtain the higher amperes required rather than the 6.6 KVA transformer used in the present work. The system can be further refined so as to make the detailed heat transfer studies in the electrode and the mould by incorporating thermocouples at these places and mass transfer studies by carefully collecting the droplets at different levels of the slag bath. Similarly the studies on the structure, segregation are the inclusions in the solidified ingots can be planned by sectioning the ingots and subjecting the same to detailed metallographic and probe analyses and the variables may include the AC or DC power supplies, polarity of the electrode, the feed rate type electrode, the flow rate of cooling water and the quantity of slag used etc.

REFERENCES

1. J. Campbell, Fluid flow and droplet formation in the ESR process, J. of Metals, July 1970, pp 23-35.

2. A. Mitchell and S. Joshi, Met. Trans., vol. 2, Feb. 1971, pp 449-455.

3. G. Hayle, Electro slag processes, principles and practice, Applied Science Publishers Ltd., 1983.

4. H. Jager, 'improved cold rolls through E S remelting', proc. of Fifth Int. Conf. on Vacuum Metallurgy and ES remelting Oct. 1976, p. 209.

5. W.R. Foley et al., Operational and economic consideration of an ESR roll building machine, Proc. of Fourth Int. Symp. on ES melting processes, June 1973, Iron and Steel Institute of Japan, Tokyo, p. 158.

6. A. Mitchell, S. Joshi and J. Cameron, Met. Trans. vol. 2, Feb. 1971, pp 561-567.

7. M.A. Maulvault, Doctoral Thesis, Dept of Metallurgy, MIT, Jan. 1971.

8. J. Mendrykowski et al., Met. Trans. ASM-AIME, 1972-3, 1761.

9. J.F. Elliott and M.A. Maulvault, Elec. Furn. Conf., Proc. AIME, 1970, 28, 13.

10. R.C. Sun and J. Pridgeon, Proc. 2nd Int. Conf. on ESR, Mellon Inst., 1969.

11. L.F. Carvajal and G.E. Geiger, Met. Trans. ASM-AIME, 1971, 2, 2087.

12. B.E. Paton, et al., 'Special Electrometallurgy', 1972, Kiev, Naukova, Dumka.

13. J.F. Elliott and J. Yavoiski: Trans. AFS, 1969, 17, 447.

14. J.P.W. Rawson, 'Slag and metal flow in electro slag remelting', Proc. of Fourth Int. Symp. on ESR, June 7-8, 1973, p. 55.

15. M. Choudhary and J. Szekely, Modelling of fluid flow and heat transfer in industrial scale ESR systems, Iron making and steel making, 8 (5), 1981, p. 225.

16. Molten Salt Chemistry, Milton Blander, Interscience Publishers, 1964.

17. S. Agarwal, Model studies on mixing and heat transfer in ESR using NH_4Cl-H_2O system, B.Tech. Thesis, IIT Kanpur, 1986.